J. Math. Biol. (2014) 68:1479–1520
DOI 10.1007/s00285-013-0664-8

Mathematical Biology

Spatiotemporal mutualistic model of mistletoes and birds

Chuncheng Wang · Rongsong Liu · Junping Shi · Carlos Martinez del Rio

Received: 23 September 2011 / Revised: 25 February 2013 / Published online: 19 April 2013

Abstract A mathematical model which incorporates the spatial dispersal and interaction dynamics of mistletoes and birds is derived and studied to gain insights of the spatial heterogeneity in abundance of mistletoes. Fickian diffusion and chemotaxis are used to model the random movement of birds and the aggregation of birds due to the attraction of mistletoes, respectively. The spread of mistletoes by birds is expressed by a dispersal operator, which is typically a convolution integral with a dispersal kernel. Two different types of kernel functions are used to study the model, one is a Dirac delta function which reflects the special case that the spread behavior is local, and the other one is a general non-negative symmetric function which describes the nonlocal spread of mistletoes. When the kernel function is taken as the Dirac delta function, the threshold condition for the existence of mistletoes is given and explored in terms of parameters. For the general non-negative symmetric kernel case, we prove the existence and stability of spatially nonhomogeneous equilibria. Numerical simulations are conducted by taking specific forms of kernel functions. Our study shows that the spatial heterogeneous patterns of mistletoes are related to the specific dispersal pattern of birds which carry mistletoe seeds.

This research is partially supported by EPSCoR start-up funds of the University of Wyoming (Liu) and NSF-US grant DMS-1022648 (Shi) .

C. Wang · R. Liu (✉)
Department of Mathematics, University of Wyoming, Laramie, WY 82071, USA
e-mail: rongsong.liu@uwyo.edu

C. Wang · C. M. del Rio
Department of Zoology and Physiology, University of Wyoming, Laramie, WY 82071, USA

C. Wang
Department of Mathematics, Harbin Institute of Technology, Harbin 150001, Heilongjiang, China

J. Shi
Department of Mathematics, College of William and Mary, Williamsburg, VA 23187-8795, USA

Keywords Mistletoe-bird dynamics · Reaction-diffusion model · Nonlocal dispersal · Delay effect · Non-constant equilibrium

Mathematics Subject Classification 92D25 · 92D40 · 37G35

Contents

1 Introduction

Animal–plant interactions often have a spatial component. Seed dispersers can change the spatial structure of plant communities and this influences the distribution of the ecological functions of the plants that they disperse (Aukema 2003; Aukema and Martinez del Rio 2002; Aukema 2004). In this paper, the interaction between mistletoes and their avian seed dispersers is qualitatively studied to explore the phenomenon of the spatial heterogeneity in abundance of mistletoes.

Mistletoes are common aerial stem-parasites that infect vascular plants ranging from pines to cacti (Kuijt 1969). Mistletoe seeds are dispersed by fruit-eating birds, many of which are highly specialized to consume their berries. Once deposited on a tree, the sticky viscin surrounding the seed adheres it to the branch, making it difficult to dislodge. After being deposited onto an appropriate host plant, a mistletoe seed germinates and forms a haustorium, tapping into the xylem of the host plant to absorb water and minerals (Calder and Bernhardt 1983). Although all mistletoes contain chlorophyll, they assimilate different amounts of organic carbon groom their hosts and range from wholly autotrophic to completely heterotrophic (Bannister and Strong 2001; Hull and Leonard 1964; Kraus et al. 1995; Marshall and Ehleringer 1990). Mistletoes are both mutualist of their animal dispersers and parasites of their host plants (del Rio et al. 1996). At the scale of individual hosts and of stands, birds respond to the presence of parasites: already parasitized hosts and stands with higher mistletoe prevalence have higher seed rain and hence have increased probability of subsequent infection (Aukema 2003; Aukema and Martinez del Rio 2002; Martinez del Rio et al. 1995; del Rio et al. 1996). Mistletoe was often considered a pest that kills trees and devalues natural habitats, but was recently recognized as an ecological keystone species, an organism that has a disproportionately pervasive influence over its community (Watson 2001). Mistletoe can have a positive effect on biodiversity by providing high quality food and habitat for a broad range of animals in forests and woodlands worldwide.

The mutualistic nature between mistletoes (the vector-borne parasites) and birds (the vectors) presents a unique opportunity to consider the interaction between parasitic and mutualistic interactions in space and time (Aukema 2003). Liu et al. (2011) proposed a deterministic model to describe the dynamics of mistletoes in an isolated patch containing an arbitrary number of plants. These plants were different in terms of mistletoe seeds deposition rate, as well as in supporting nutrition for the parasites. A Holling type II functional response was used to model the process that fruits were removed by birds. It was assumed in the model that either birds removed fruits from plants without any bias or with preference for certain types of plants. After a bird removed seeds from mistletoes, it was assumed that the bird distributed the seeds randomly among plants. Concrete criterions, expressed in terms of the model parameters, for mistletoes establishing in the area were derived analytically. Since the models in Liu et al. (2011) were built in an isolated area, birds were assumed to be constant in this area. In reality, the number of birds might change according to the food availability, and the dynamics of birds and mistletoes are interdependent with each other. In order to better understand the interaction between mistletoes and their avian seed dispersers, we incorporate the dynamics of the bird population into the mistletoe model. In this paper, we describe the interaction of mistletoes and avian seed dispersers using a dynamic model which incorporates the spatial dispersal of birds, birds' reaction to the presence of parasites, the maturation duration of mistletoes, the fruit removal process, and the fruit distributed by birds.

We assume that, without mistletoes, the bird population satisfies a logistic growth model since birds have other food items available besides of mistletoes (Murphy and Kelly 2003; Walsberg 1975). The spatial dispersal of birds is described in two ways. First the random movement of birds in the habitat is modeled with a Fickian diffusion of the bird population. Secondly we assume that birds make directed dispersal based on the density of mistletoes (their food resource), which is described through chemotactic advection. The additional growth of bird population due to consuming mistletoes is assumed to be proportional to the predation rate of birds on mistletoes. This additional growth depends on the dispersal pattern of birds, and the growth at a location x depends on seed dropping from birds from all possible locations y. Such spatial dependent growth is characterized by a linear continuous mapping K, which describes the seed spatial redistribution by the birds. The mapping K is typically a convolution integral of the local mistletoe consumption rate of birds and a dispersal kernel function $k(x, y)$, and the local-only redistribution is also included as it can be thought as a Dirac delta kernel function or an identity map $K[u] = u$. Vice versa, the same dispersal mapping is used for the growth of the mistletoe as birds drop seeds while flying a similar dispersal pattern. Similar to Liu et al. (2011), the maturation time is included in the mistletoe growth equation as a time-delay and also a decay factor. The matured mistletoes grow on trees, and they do not move spatially. Our model derivation is described in detail in Sect. 2, where detailed biological explanations of all the terms involved are provided and also the corresponding dimensionless model is given.

In Sect. 3, the global existence, boundedness and uniqueness of solutions of the proposed model without chemotactic effect is proved, hence the model is well-posed in this case. In Sect. 4, the model is analyzed under the assumption that the dispersal

of mistletoes by birds is local only. In this special case, the dispersal mapping is a simple identity map. If the spreading of mistletoes by birds is nonlocal, a more general dispersal mapping which is compact and strongly positive is used to study the model. In Sect. 5, the existence and stability of nonconstant equilibrium solutions of the model with general dispersal mapping is shown, which could explain the spatial heterogeneity of mistletoes distribution. In Sect. 6, numerical simulations are conducted by taking some specific forms of dispersal mappings which illustrate and reinforce the analytical results. Concluding remarks are given in the final section.

2 Derivation of the model

Let $M(t,x)$ denote the density of adult mistletoes and let $B(t,x)$ denote the density of birds under consideration at time t and location $x \in \Omega$. Here Ω, the habitat for mistletoes and birds, is a bounded connected open subset of $\mathbb{R}^n$ ($n \geq 1$) with smooth boundary $\partial\Omega$. The domain Ω consists of uniformly grown trees where mistletoes attach to.

First, we derive the equation for the density of adult mistletoes $M(t,x)$. After a mistletoe seed attaches to a branch, it takes several years for this seed to germinate, grow and mature. The maturation duration of mistletoes can be considered by an age-structured equation as follows. Let $m(t,a,x)$ denote the density of mistletoes with age a. Then a standard argument of population with age structure (Metz and Diekmann 1983) gives

$$\frac{\partial m(t,a,x)}{\partial t} + \frac{\partial m(t,a,x)}{\partial a} = -d(a,x)m(t,a,x), \tag{1}$$

where $d(a,x)$ is the age related death rate of mistletoes. Let τ denote the maturation time of mistletoes, then the density of adult mistletoes at time t and location x is given by

$$M(t,x) = \int_{\tau}^{\infty} m(t,a,x)da.$$

Therefore,

$$\begin{aligned}\frac{\partial M(t,x)}{\partial t} &= \int_{\tau}^{\infty} \frac{\partial m(t,a,x)}{\partial t} da \\ &= \int_{\tau}^{\infty} \left(-\frac{\partial m(t,a,x)}{\partial a} - d(a,x)m(t,a,x) \right) da \\ &= m(t,\tau,x) - d_m(x)M(t,x),\end{aligned}$$

where we make the biological realistic assumption that $m(t, \infty, x) = 0$ and the age specific death rate is

$$d(a, x) = \begin{cases} d_i(x), & a < \tau, \\ d_m(x), & a > \tau. \end{cases}$$

Only adult mistletoes can produce fruits and fruits are dispersed by birds to be attached to a tree.

The relationship between mistletoes' berries and birds belongs to a resource–consumer interaction. Then the resource-dependent consumption rate of mistletoes by birds at location x and time t is $f(M(t, x))B(t, x)$, where $f(M)$ is the predator functional response. We assume that f satisfies a Holling type growth rate:

(f) $f \in C^1(\mathbb{R}^+)$, $f(0) = 0$, $f'(M) > 0$ for $M \geq 0$, and $\lim_{M\to\infty} f(M) = f_\infty$.

Since the birds move in the habitat Ω, then the consumption of berries at a location x may not directly result in growth of birds at the same spatial location, and for the same reason, birds may drop berry seeds eaten at location x to a different location y. Hence following Liu et al. (2011), the birth rate of mistletoes at $x \in \Omega$ is given by

$$m(t, 0, x) = \alpha(x)K[f(M(t, \cdot))B(t, \cdot)], \tag{2}$$

where $\alpha(x)$ is the successful attachment rate of a mistletoe seed to a tree, and K is a linear continuous mapping which maps a continuous function defined in $\overline{\Omega}$ to another continuous function defined in $\overline{\Omega}$. The mapping $u(x) \mapsto K[u](x)$ can be interpreted as a redistribution of a continuous density function $u(x)$, which depicts the redistribution of the berry seeds due to the bird dispersal. More often people have used an integral representation

$$K[u](x) = \int_\Omega k(x, y)u(y)dy,$$

and the kernel function $k(x, y)$ describes the dispersal of mistletoes fruit by birds from location y to location x. The following two cases are often considered:

$(H1)$ $k(x, y) = \delta_x(y)$, where $\delta_x(y)$ is the Dirac delta function which satisfies

$$\int_{-\infty}^{\infty} \delta_x(y)g(y)dy = g(x),$$

for any smooth function g with compact support; or

$(H2)$ $k(x, y) \in C(\overline{\Omega} \times \overline{\Omega}, \mathbb{R}^+)$, $k(y, x) = k(x, y)$ and $k(x, y) \geq 0$ for $(x, y) \in \overline{\Omega} \times \overline{\Omega}$.

Note that $(H1)$ is $K[u] = u$, the identity mapping, and the dispersal is "local", while $(H2)$ gives a nonlocal dispersal pattern. To accommodate both and more general dispersal patterns, we use the formulation in (2). We assume that $K : C(\overline{\Omega}) \to C(\overline{\Omega})$ is a linear mapping satisfying

$(K1)$ $||K[u]||_{C(\overline{\Omega})} \le A_1||u||_{C(\overline{\Omega})}$ for some $A_1 > 0$;

$(K2)$ If $u(x) \ge 0$ for all $x \in \overline{\Omega}$, then for $0 \le C_1 < C_2$, $K[C_1u](x) \le K[C_2u](x)$ for $x \in \overline{\Omega}$, and

$$K[u](x) \le A_2 \max\left\{u(x), \int_{\Omega} u(x)dx\right\}, \tag{3}$$

for some $A_2 > 0$.

Note that the boundedness assumption in $(K1)$ implies that K is continuous. The assumption $(K2)$ implies that K is order-preserving and K is also bounded pointwisely.

Now to obtain an equation for the density of adult mistletoes, we can calculate $m(t, \tau, x)$ by integrating (1) along the characteristic, and we have

$$m(t, \tau, x) = \alpha(x)e^{-d_i(x)\tau}K[f(M(t-\tau, \cdot))B(t-\tau, \cdot)](x). \tag{4}$$

Hence, the density of adult mistletoes population satisfies

$$\frac{\partial M(t, x)}{dt} = \alpha(x)e^{-d_i(x)\tau}K[f(M(t-\tau, \cdot))B(t-\tau, \cdot)](x) - d_m(x)M(t, x). \tag{5}$$

For the bird population, since birds have other food resource besides mistletoe fruits, we assume that without mistletoes, the bird population has a logistic growth rate $g(B)$ which satisfies

(g) $g \in C^1(\mathbb{R}^+)$, $g(0) = g(K_B) = 0$, $g(B) > 0$ in $(0, K_B)$, and $g(B) < 0$ for $B > K_B$.

With the additional food source of the mistletoes, the bird population gets a further increase, and the rate of the increase is proportional to mistletoe fruits eaten by birds. Again this increase is described by $K[f(M(t, \cdot))B(t, \cdot)]$.

For the spatial movement of the birds, we first assume that birds disperse along the habitat randomly, and the dispersal is modeled with Fickian diffusion. And in addition to the random movement, we also assume that birds are attracted by trees with more mistletoes, hence a chemotactic type advection is included in the equation. In summary, we have the following equation to describe the bird population:

$$\begin{aligned}\frac{\partial B(t, x)}{\partial t} &= D\Delta B(t, x) - \nabla(\beta B(t, x)\nabla M(t, x)) + g(B(t, x)) \\ &\quad + cK[f(M(t, \cdot))B(t, \cdot)](x),\end{aligned} \tag{6}$$

where D is the diffusion coefficient of birds, β is the chemotactic coefficient, and c is the conversion rate from mistletoes fruits birds eaten into birds population. Note that here we assume that $c \ge 0$ as the bird population may not increase by eating mistletoe berries and in that case the birds serve as a pure carrier.

We now equip the model (5) and (6) with the following initial data:

$$\begin{aligned} M(\theta, x) &= M_0(\theta, x) \geq 0, \quad \text{for } \theta \in [-\tau, 0],\ x \in \Omega, \\ B(\theta, x) &= B_0(\theta, x) \geq 0, \quad \text{for } \theta \in [-\tau, 0],\ x \in \Omega, \end{aligned} \tag{7}$$

where $M_0(\theta, x)$ and $B_0(\theta, x)$ are prescribed continuous functions with respect to variables $\theta \in [-\tau, 0]$ and $x \in \Omega$. We also impose a no-flux boundary condition for the bird equation:

$$[D\nabla B(t, x) - \beta B(t, x)\nabla M(t, x)] \cdot n(x) = 0, \quad \text{for } t > 0,\ x \in \partial\Omega, \tag{8}$$

where $n(x)$ is the outer normal vector at $x \in \partial\Omega$. This boundary condition shows that the movement of birds is restricted in the habitat Ω, which is then a closed environment. No boundary condition is imposed for the mistletoe population as the value of $M(t, x)$ is determined by the equation pointwisely. From numerical simulations in Sect. 6, the boundary value of $M(t, x)$ may depend on the dispersal mapping.

The resulting mathematical model is a reaction-diffusion-advection equation with nonlocal growth for the bird population, coupled with a nonlocal delay differential equation for mistletoes with no spatial movement. The contrasting mathematical properties of the two equations make the whole system a distinctive one which contains diffusion, advection, time-delay and nonlocal effect. Mathematical modeling and analysis of ecological systems involving both time delay and diffusion have been considered by many investigators, see surveys by Gourley et al. (Gourley et al. 2004; Gourley and Wu 2006). In particular, the nonlocality of the delay effect has been recognized and appropriately incorporated into the spatiotemporal models. Our model here provides another example of ecological models with complex interaction and dispersal behavior. Our mathematical result supports the heterogenous spatial distribution of mistletoes found in the field studies (Aukema and Martinez del Rio 2002; Aukema 2004), and it also shows the effect of chemotaxis-induced directed dispersal to the dynamics and spatial patterns.

3 Existence, bounds and uniqueness of solutions

In this section, we consider the existence of solutions to the proposed model equipped with the initial condition (7) and the no-flux boundary condition for the bird Eq. (8). Hence the whole system is given by

$$\begin{cases} \dfrac{\partial M}{\partial t} = \alpha e^{-d_i\tau} K[f(M(t-\tau,\cdot))B(t-\tau,\cdot)] - d_m M & x \in \overline{\Omega}, t > 0, \\ \dfrac{\partial B}{\partial t} = D\Delta B - \nabla(\beta B \nabla M) + g(B) + cK[f(M(t,\cdot))B(t,\cdot)], & x \in \Omega, t > 0, \\ M(t, x) = M_0(t, x),\ B(t, x) = B_0(t, x), & x \in \Omega, -\tau \leq t \leq 0, \\ [D\nabla B(t, x) - \beta B(t, x)\nabla M(t, x)] \cdot n(x) = 0, & x \in \partial\Omega, \end{cases} \tag{9}$$

where $M = M(t, x)$ and $B = B(t, x)$. Here, Ω is a bounded domain in $\mathbb{R}^n$ ($n \geq 1$) with smooth boundary $\partial\Omega$; the mapping/functions K, f, g satisfy $(K1) - (K2)$,

(f) and (g) respectively; the parameters satisfy $D > 0, c \geq 0, \tau \geq 0$ and $\beta \geq 0$; and

$$\alpha(x) \geq \alpha_0 > 0, \quad d_i(x) \geq d_i^0 > 0, \quad d_m(x) \geq d_m^0 > 0, \quad x \in \overline{\Omega}. \tag{10}$$

We aim to prove the existence, boundedness, and uniqueness of globally defined solutions to (9) under the assumption of $\beta = 0$ (without the chemotactic effect). For $\beta = 0$, we rewrite (9) in the following form

$$\begin{pmatrix} \frac{\partial M}{\partial t} \\ \frac{\partial B}{\partial t} \end{pmatrix} = A \begin{pmatrix} M \\ B \end{pmatrix} + V \begin{pmatrix} M_t \\ B_t \end{pmatrix}, \tag{11}$$

where

$$A = \begin{pmatrix} 0 & 0 \\ 0 & D\Delta \end{pmatrix},$$

and

$$V \begin{pmatrix} M_t \\ B_t \end{pmatrix} = \begin{pmatrix} \alpha e^{-d_i \tau} K[f(M(t-\tau,\cdot))B(t-\tau,\cdot)] - d_m M \\ g(B) + cK[f(M(t,\cdot))B(t,\cdot)] \end{pmatrix}.$$

Here M_t and B_t, due to the time delay, are functions of θ and x and are defined by

$$M_t(\theta, x) = M(t+\theta, x), \quad B_t(\theta, x) = B(t+\theta, x), \quad t \in [-\tau, 0], \ x \in \overline{\Omega}.$$

The proper phase space of (11) can be chosen as

$$X \times Y := C([-\tau, 0], C(\overline{\Omega})) \times C([-\tau, 0], C_n^{2,\gamma}(\overline{\Omega})),$$

where $C_n^{2,\gamma}(\overline{\Omega}) := \{v \in C^{2,\gamma}(\overline{\Omega}) : \frac{\partial v}{\partial n} = 0\}$ with $\gamma \in (0, 1)$. Note here since $\beta = 0$, then the boundary condition for the bird population becomes a Neumann one: $\nabla B = 0$. Let $Q_t : X \times Y \to X \times Y$ be

$$Q_t(\phi)(x) = (M_t(\theta, x, \phi), B_t(\theta, x, \phi)), \quad \theta \in [-\tau, 0], \ x \in \overline{\Omega}, \ \phi \in X \times Y, \tag{12}$$

where $(M(t, x, \phi), B(t, x, \phi))$ is the solution of the system (11). Then Q_t is locally well defined and can be globally extended to $t \in (0, \infty)$ in view of the next theorem.

Theorem 3.1 *Assume that $\beta = 0$, the mapping/functions K, f, g satisfy $(K1) - (K2)$, (f) and (g) respectively, the parameters satisfy $D > 0, c \geq 0, \tau \geq 0$ and $\beta \geq 0$, and $\alpha(x), d_i(x), d_m(x)$ satisfy (10). Then for any $\phi = (\phi_{10}(\theta, x), \phi_{20}(\theta, x)) \in X \times Y$, the system (9) has a unique mild solution $(M(t, x), B(t, x))$ with initial value ϕ, where $M(t, x)$ and $B(t, x)$ are defined on $[-\tau, \infty) \times \overline{\Omega}$. Moreover, if $\phi_{10}(\theta, x) \geq 0$ and $\phi_{20}(\theta, x) \geq 0$ on $[-\tau, 0] \times \overline{\Omega}$, then $M(t, x) \geq 0$ and $B(t, x) \geq 0$ for any $t > 0, x \in \overline{\Omega}$.*

Proof The existence of a unique local mild solution of (11) is the consequence of Theorem 1 in Martin and Smith (1990). The positivity of solutions with nonnegative initial values follows from the quasi-monotonicity of V. We notice that from condition (g), there exists $g_1 > 0$ and $K_B > 0$ such that

$$g(B) \leq g_1 B(K_B - B), \quad B \in \mathbb{R}^+. \tag{13}$$

Define $\mathcal{B}(t) = \int_\Omega B(t,x)dx$. From (11), (13), $(K2)$, Cauchy-Schwarz inequality and the Neumann boundary condition, we obtain that

$$\begin{aligned}
\frac{d\mathcal{B}(t)}{dt} &\leq \int_\Omega \left[D\Delta B + g_1 B(K_B - B) + \int_\Omega c f_\infty K[B(t,\cdot)](x)dx \right] dx \\
&\leq g_1 K_B \int_\Omega B(t,x)dx - \frac{g_1}{|\Omega|}\left(\int_\Omega B(t,x)dx \right)^2 \\
&\quad + cA_2 f_\infty \int_\Omega \max\left\{ B(t,x), \int_\Omega B(t,y)dy \right\} dx \\
&\leq g_1 K_B \mathcal{B} - \frac{g_1}{|\Omega|}\mathcal{B}^2 + cA_2 f_\infty (1+|\Omega|)\mathcal{B} \\
&= \mathcal{B}\left(cA_2 f_\infty (1+|\Omega|) + g_1 K_B - \frac{g_1}{|\Omega|}\mathcal{B} \right).
\end{aligned} \tag{14}$$

From the inequality satisfied by $\mathcal{B}$, we conclude that

$$\limsup_{t\to\infty} \mathcal{B}(t) = \limsup_{t\to\infty} \int_\Omega B(t,x)dx \leq \frac{(cA_2 f_\infty (1+|\Omega|) + g_1 K_B)|\Omega|}{g_1} := A_3. \tag{15}$$

This indicates that $B(t,x)$ has an L^1 *a priori* estimate A_3. Next we follow a similar approach as in Alikakos (1979a,b) to prove that $B(t,x)$ is bounded in $L^\infty(\Omega)$ for all $t > 0$.

Multiplying the second equation of (9) by B^s, $(s > 0)$ and integrating over Ω, we get that for $t > 0$,

$$\begin{aligned}
\frac{1}{s+1}\frac{d}{dt}\int_\Omega B^{s+1}dx &\leq D\int_\Omega B^s \Delta B dx + g_1 K_B \int_\Omega B^{s+1}dx - g_1 \int_\Omega B^{s+2}dx \\
&\quad + c\int_\Omega B^s K[f(M(t,\cdot))B(t,\cdot)](x)dx \\
&\leq -Ds\int_\Omega B^{s-1}|\nabla B|^2 dx + g_1 K_B \int_\Omega B^{s+1}dx - g_1 \int_\Omega B^{s+2}dx
\end{aligned}$$

$$
\begin{aligned}
&+cA_2 f_\infty \int_\Omega B^s \max\left\{B(t,x), \int_\Omega B(t,y)dy\right\} dx \\
&\le -Ds\int_\Omega B^{s-1}|\nabla B|^2 dx + g_1 K_B \int_\Omega B^{s+1}dx - g_1\int_\Omega B^{s+2}dx \\
&+cA_2 f_\infty\left(\int_\Omega B^{s+1}dx + \mathcal{B}\int_\Omega B^s dx\right). \qquad (16)
\end{aligned}
$$

We notice that

$$
\int_\Omega B^{s-1}|\nabla B|^2 dx = \frac{4}{(s+1)^2}\int_\Omega |\nabla(B^{\frac{s+1}{2}})|^2 dx. \qquad (17)
$$

Denote the average of u over Ω by $\overline{u}$. It follows by Poincaré's inequality that there exists a constant C_1, depending only on Ω, such that

$$
\begin{aligned}
C_1\int_\Omega |\nabla(B^{\frac{s+1}{2}})|^2 dx &\ge \int_\Omega (B^{\frac{s+1}{2}} - \overline{B^{\frac{s+1}{2}}})^2 dx \\
&= \int_\Omega B^{s+1}dx + \left(\frac{1}{|\Omega|^2} - \frac{2}{|\Omega|}\right)\left(\int_\Omega B^{\frac{s+1}{2}}dx\right)^2. \qquad (18)
\end{aligned}
$$

Combining (15), (16), (17), and (18) and using Hölder inequality, we have, for a small $\delta > 0$, there exists $T_1 > 0$ such that when $t > T_1$,

$$
\begin{aligned}
&\frac{1}{s+1}\frac{d}{dt}\int_\Omega B^{s+1}dx \\
&\le -\frac{4Ds}{(s+1)^2}\int_\Omega |\nabla(B^{\frac{s+1}{2}})|^2 dx + (g_1K_B + cA_2f_\infty)\int_\Omega B^{s+1}dx \\
&\quad -g_1\int_\Omega B^{s+2}dx + cA_2(A_3+\delta)f_\infty\int_\Omega B^s dx \\
&\le -\frac{4Ds}{C_1(s+1)^2}\left(\int_\Omega B^{s+1}dx + \left(\frac{1}{|\Omega|^2} - \frac{2}{|\Omega|}\right)\left(\int_\Omega B^{\frac{s+1}{2}}dx\right)^2\right) \\
&\quad +(g_1K_B + cA_2f_\infty)\int_\Omega B^{s+1}dx - g_1\int_\Omega B^{s+2}dx + cA_2(A_3+\delta)f_\infty\int_\Omega B^{s+1}dx \\
&\le \frac{4Ds}{C_1(s+1)^2}\int_\Omega B^{s+1}dx + (g_1K_B + cA_2f_\infty)\int_\Omega B^{s+1}dx
\end{aligned}
$$

$$-g_1\left(\frac{1}{|\Omega|^{\frac{1}{s+2}}}\int_\Omega B^{s+1}dx\right)^{\frac{s+2}{s+1}}+cA_2(A_3+\delta)f_\infty\int_\Omega B^{s+1}dx$$
$$=\left(C_2(s)-C_3(s)\left(\int_\Omega B^{s+1}dx\right)^{\frac{1}{s+1}}\right)\int_\Omega B^{s+1}dx, \tag{19}$$

where

$$C_2(s)=\frac{4Ds}{C_1(s+1)^2}+(g_1K_B+cA_2f_\infty)+cA_2(A_3+\delta)f_\infty,$$
$$C_3(s)=g_1|\Omega|^{-\frac{1}{s+1}}.$$

Therefore,

$$\limsup_{t\to\infty}\left(\frac{1}{|\Omega|}\int_\Omega B^{s+1}dx\right)^{\frac{1}{s+1}}\le\frac{C_2(s)}{g_1},$$

which implies that

$$\limsup_{t\to\infty}\|B(t,\cdot)\|_{L^\infty(\Omega)}=\limsup_{t\to\infty}\lim_{s\to\infty}\left(\frac{1}{|\Omega|}\int_\Omega B^{s+1}dx\right)^{\frac{1}{s+1}}$$
$$\le\lim_{s\to\infty}\frac{C_2(s)}{g_1}=\frac{(g_1K_B+cA_2f_\infty)+cA_2(A_3+\delta)f_\infty}{g_1}. \tag{20}$$

Finally, as the constant $\delta>0$ can be chosen arbitrarily, then the upper bound in (20) can be chosen as

$$A_4:=\frac{g_1K_B+cA_2f_\infty+cA_2A_3f_\infty}{g_1}.$$

On the other hand, for $t>T_1$, we have

$$\frac{\partial M}{\partial t}=-d_mM+\alpha e^{-d_i\tau}K[f(M(t-\tau,\cdot))B(t-\tau,\cdot)](x)$$
$$\le-d_mM+\alpha e^{-d_i\tau}f_\infty\max\{A_3,A_4\}. \tag{21}$$

Hence, there exists $T_2>T_1$ such that $M(t,x)<\dfrac{\alpha e^{-d_i\tau}f_\infty\max\{A_3,A_4\}}{d_m}$ for $t>T_2, x\in\overline{\Omega}$. By using Sobolev embedding theorem, we also obtain the bounededness of $B(t,x)$ in Y. The boundedness of $M(t,x)$ and $B(t,x)$ imply the global existence of the solution, which completes the proof. □

Remark 3.2 1. The estimates in the proof of Theorem 3.1 provide explicit bounds for the solution $(M(t,x), B(t,x))$:

$$\begin{aligned} \limsup_{t\to\infty} M(t,x) &\le \frac{\alpha e^{-d_i\tau} f_\infty \max\{A_3, A_4\}}{d_m}, \\ \limsup_{t\to\infty} B(t,x) &\le \frac{g_1 K_B + cA_2 f_\infty + cA_2 A_3 f_\infty}{g_1} := A_4, \\ A_3 &:= \frac{(cA_2 f_\infty(1+|\Omega|) + g_1 K_B)|\Omega|}{g_1}. \end{aligned} \tag{22}$$

Clearly the bounds in (22) are also satisfied by any equilibria of the system (9). When the conversion rate $c = 0$, then $A_3 = K_B|\Omega|$ and $A_4 = K_B$, so in that case, the bounds are basically provided by the carrying capacity.

2. The global-in-time existence of the solution to (9) with chemotactic effect ($\beta > 0$) is not known, even for most simpler chemotaxis systems (Hillen and Painter 2009; Horstmann and Winkler 2005).

Theorem 3.1 ensures the well-posedness and global existence of solutions of our model (9) under general conditions (f), (g) and $(K1)$–$(K2)$. For an in-depth analysis of the model, we choose more specific f and g with more biological parameters, which are derived from the concrete biological processes, see Liu et al. (2011) for more details. From now on, we assume that

$$f(M) = \frac{a\sigma sM}{1 + ha\sigma sM}, \quad g(B) = rB\left(1 - \frac{B}{K_B}\right). \tag{23}$$

The functional form of $f(M)$ is the classical Holling type II functional response (Holling 1959a,b). Here sM denotes the total number of fruits produced by the adult mistletoes; a is the encounter rate per fruit for a bird, σ is the consumption choice coefficient of a bird, meaning whether the bird eats or not when it meets a fruit, and h denotes the handling time the bird spends on one fruit. The bird population satisfies a logistic growth model with the intrinsic growth rate r and the carrying capacity K_B.

We also assume that $\alpha(x) = \alpha$, $d_i(x) = d_i$, and $d_m(x) = d_m$, and define dimensionless variables:

$$\bar{M} = a\sigma sM, \quad \bar{B} = \frac{B}{N}, \quad \text{and } \bar{t} = rt,$$

and new parameters

$$\bar{\alpha} = \frac{a\sigma sK_B\alpha}{rh}, \quad w = \frac{1}{h}, \quad \bar{d}_m = \frac{d_m}{r}, \quad \bar{D} = \frac{D}{r}, \quad \bar{\beta} = \frac{\beta a\sigma s}{r}, \quad \bar{c} = \frac{c}{rh}. \tag{24}$$

Then by dropping the bars for the variables and parameters in equations, the model (9) can be rewritten as a new dimensionless model

$$\begin{cases} \dfrac{\partial M}{\partial t} = \alpha e^{-d_i \tau} K\left[\dfrac{M(t-\tau,\cdot)}{M(t-\tau,\cdot)+w} B(t-\tau,\cdot)\right] - d_m M(t,x), \\ \dfrac{\partial B}{\partial t} = D\Delta B - \beta\nabla(B\nabla M) + B(1-B) + cK\left[\dfrac{M(t,\cdot)}{M(t,\cdot)+w} B(t,\cdot)\right]. \end{cases} \tag{25}$$

4 Analysis of the model with a Dirac delta kernel function

In this section, we will analyze the system (25), under the assumption $(H1)$, that is, the dispersal mapping $K[u] = u$ is an identity map, or equivalently, the kernel function $k(x, y)$ is a Dirac delta function. Hence the dispersal of mistletoe fruits by birds is local only, not over a longer range. Under this assumption, the system (25) takes the form:

$$\begin{cases} \dfrac{\partial M}{\partial t} = \alpha e^{-d_i \tau} \dfrac{M(t-\tau,x)B(t-\tau,x)}{M(t-\tau,x)+w} - d_m M, & x \in \overline{\Omega}, t > 0, \\ \dfrac{\partial B}{\partial t} = D\Delta B - \beta\nabla(B\nabla M) + B(1-B) + \dfrac{cMB}{M+w}, & x \in \Omega, t > 0, \\ M(t,x) = M_0(t,x), B(t,x) = B_0(t,x), & x \in \Omega, -\tau \le t \le 0, \\ [D\nabla B(t,x) - \beta B(t,x)\nabla M(t,x)] \cdot n(x) = 0, & x \in \partial\Omega, \end{cases} \tag{26}$$

where $M = M(t, x)$ and $B = B(t, x)$. In Sect. 4.1, we classify all constant equilibria of (26), and the stability of these equilibria without spatial structure and delay effect is analyzed in Sect. 4.2. The effect of time delay (but still without spatial structure) is considered in Sect. 4.3, and finally in Sect. 4.4, the stability of constant equilibria with respect to the dynamics of (26) is analyzed.

4.1 Constant equilibria

The constant equilibria of the model (26) are determined by the following system:

$$\begin{cases} \alpha e^{-d_i \tau} \dfrac{M}{M+w} B - d_m M = 0, \\ B(1-B) + \dfrac{cMB}{M+w} = 0. \end{cases} \tag{27}$$

Solving the above equations, we have the trivial equilibria $E_0 = (0, 0)$, $E_1 = (0, 1)$, or the positive constant equilibria satisfying

$$B = 1 + \frac{cM}{M+w}, \tag{28}$$

and

$$\xi_\tau(M+w) = 1 + \frac{cM}{M+w}, \tag{29}$$

where $\xi_\tau = d_m \alpha^{-1} e^{d_i \tau}$. Let $P = M + w$, then the Eq. (29) can be rewritten as

$$\xi_\tau P^2 - (1+c)P + cw = 0. \tag{30}$$

We can see that if the determinant of the above quadratic equation is nonnegative, *i.e.*,

$$\Delta := (1+c)^2 - 4cw\xi_\tau \geq 0, \tag{31}$$

or

$$d_m \leq \frac{(1+c)^2\alpha}{4cwe^{d_i\tau}}, \tag{32}$$

(30) has two real roots. Denote the solutions of (30) as

$$P_\pm^\tau = \frac{1+c \pm \sqrt{\Delta}}{2\xi_\tau}.$$

So, if d_m satisfies (32), the model has two constant equilibria $E_\pm^\tau = (M_\pm^\tau, B_\pm^\tau)$ with $M_\pm^\tau = P_\pm^\tau - w$ and $B_\pm^\tau = 1 + \frac{cM_\pm^\tau}{M_\pm^\tau + w}$. These two equilibria are not necessarily positive.

Notice that (29) can be rewritten as

$$d_m = \frac{\alpha(M+w+cM)}{(M+w)^2 e^{d_i\tau}} := h_1(M).$$

Hence if we use d_m as a bifurcation parameter, and we can define two bifurcation values:

$$d_{m,\tau}^* = \frac{(1+c)^2\alpha}{4cwe^{d_i\tau}}, \quad \text{and} \quad \widetilde{d}_{m,\tau} = \frac{\alpha}{e^{d_i\tau}w}. \tag{33}$$

Here $d_{m,\tau}^*$ is a saddle-node bifurcation point, and $\widetilde{d}_{m,\tau} = h_1(0)$ is a transcritical bifurcation point where a curve of nontrivial solutions intersects with the line of trivial solutions $(d_m, M, B) = (d_m, 0, 1)$. It is easy to calculate that $h_1'(0) = \frac{\alpha(c-1)}{w^2 e^{d_i\tau}}$, and that $h_1(M)$ has at most one critical point at $\widetilde{M} = \frac{w(c-1)}{1+c}$ if $c > 1$. Define

$$M_\pm^\tau = \frac{1+c \pm \sqrt{(1+c)^2 - 4cw\xi_\tau}}{2\xi_\tau} - w, \quad \text{and} \quad B_\pm^\tau = 1 + c\frac{M_\pm^\tau}{M_\pm^\tau + w}. \tag{34}$$

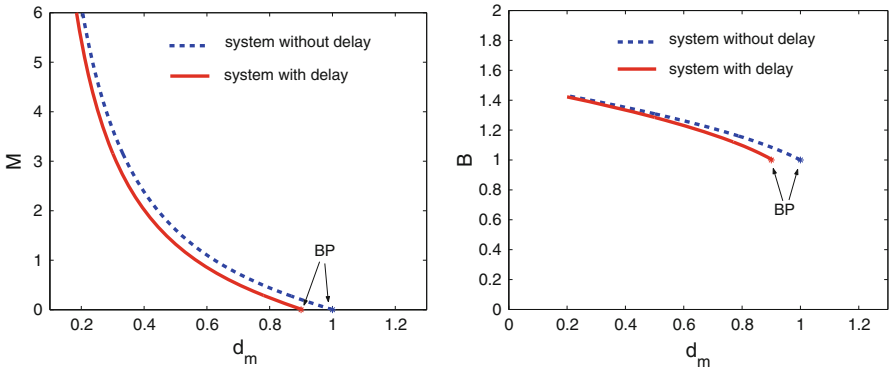

Fig. 1 Bifurcation diagram of (27) for $\tau = 0$ (*dashed blue*) and $\tau = 1$ (*solid red*). Here $w = 1, \alpha = 1, c = 0.5$. The *horizontal axis* is the parameter d_m, and the *vertical axis* is M (*left*) and B (*right*)

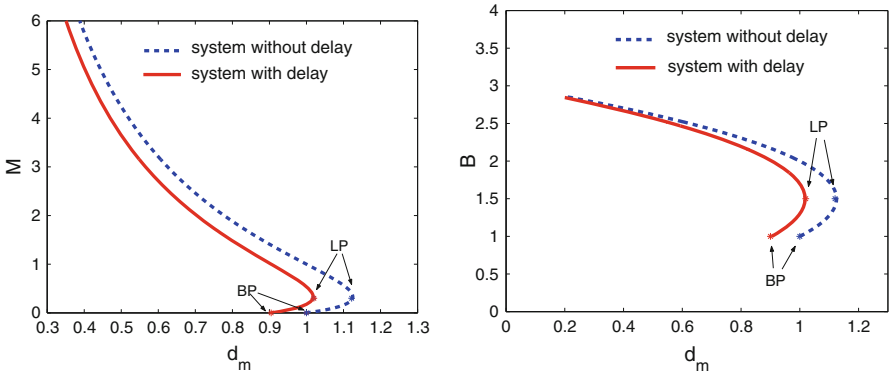

Fig. 2 Bifurcation diagram of (27) for $\tau = 0$ (*dashed blue*) and $\tau = 1$ (*solid red*). Here $w = 1, \alpha = 1, c = 2$. The *horizontal axis* is the parameter d_m, and the *vertical axis* is M (*left*) and B (*right*)

Hence we have the following two cases for the global bifurcation of the positive constant equilibria:

1. If $0 \leq c \leq 1$, then the transcritical bifurcation at $(\widetilde{d}_{m,\tau}, 0, 1)$ is subcritical for the positive branch. For $d_m > \widetilde{d}_{m,\tau}$, there is no positive constant equilibria; for $d_m \in (0, \widetilde{d}_{m,\tau}]$, (26) has a unique positive constant equilibrium given by $E_+^\tau = (M_+^\tau, B_+^\tau)$. (see Fig. 1)
2. If $c > 1$, then the transcritical bifurcation at $(\widetilde{d}_{m,\tau}, 0, 1)$ is supercritical for the positive branch, and a saddle-node bifurcation occurs at $d_m = d_{m,\tau}^* > \widetilde{d}_{m,\tau}$. For $d_m > d_{m,\tau}^*$, there is no positive constant equilibrium; for $d_m \in (\widetilde{d}_{m,\tau}, d_{m,\tau}^*]$, there are exactly two positive constant equilibria of the model (26), $E_\pm^\tau = (M_\pm^\tau, B_\pm^\tau)$; for $d_m \in (0, \widetilde{d}_{m,\tau}]$, there is only one positive constant equilibrium $E_+^\tau = (M_+^\tau, B_+^\tau)$. (see Fig. 2)

4.2 Linearized stability analysis I: without delay effect and without spatial structure

We first examine the stability of the constant equilibria in the dynamics without the delay effect and without the spatial structure. That is, we aim to see the dynamics of the model (26) with the delay $\tau = 0$ and the spatial domain $\Omega = \{$ one point $\}$. Then the system (26) effectively becomes a system of nonlinear ODEs:

$$\begin{cases} M' = \dfrac{\alpha M B}{M + w} - d_m M, \\ B' = B(1 - B) + \dfrac{c M B}{M + w}. \end{cases} \tag{35}$$

The equilibria of (35) have been analyzed in the last subsection.

The Jacobian matrix of the system (35) at an equilibrium $E^* = (M^*, B^*)$ is given by

$$J(E^*) = \begin{pmatrix} \dfrac{\alpha w B^*}{(M^* + w)^2} - d_m & \dfrac{\alpha M^*}{M^* + w} \\ \dfrac{c w B^*}{(M^* + w)^2} & 1 - 2B^* + \dfrac{c M^*}{M^* + w} \end{pmatrix}.$$

At $(0, 0)$, we have

$$J((0, 0)) = \begin{pmatrix} -d_m & 0 \\ 0 & 1 \end{pmatrix}.$$

Therefore, the origin is always a saddle.

At $(0, 1)$, we have

$$J((0, 1)) = \begin{pmatrix} -d_m + \dfrac{\alpha}{w} & 0 \\ \dfrac{c}{w} & -1 \end{pmatrix}.$$

We can see that if $d_m > \dfrac{\alpha}{w}$, then $(0, 1)$ is stable; if $d_m < \dfrac{\alpha}{w}$, then $(0, 1)$ is a saddle.

For the interior equilibrium $(M_\pm^0, B_\pm^0)$, combining (28) and (29) for $\tau = 0$, we have

$$J((M_\pm^0, B_\pm^0)) = \begin{pmatrix} \dfrac{-d_m M_\pm^0}{M_\pm^0 + w} & \dfrac{\alpha M_\pm^0}{M_\pm^0 + w} \\ \dfrac{c w B_\pm^0}{(M_\pm^0 + w)^2} & -B_\pm^0 \end{pmatrix}.$$

The trace of the above Jacobian matrix is given by

$$\text{Trace} = \frac{-d_m M_\pm^0}{M_\pm^0 + w} - B_\pm^0 < 0,$$

if $M_\pm^0 > 0$. This means that there is no Hopf bifurcation at the interior equilibrium.

On the other hand, the determinant of the Jacobian matrix $J((M_\pm^0, B_\pm^0))$ can be calculated as

$$\begin{aligned}\text{Det} &= \frac{B_\pm^0 M_\pm^0}{M_\pm^0 + w}\left(d_m - \frac{cw\alpha}{(M_\pm^0 + w)^2}\right)\\ &= \frac{B_\pm^0 M_\pm^0}{M_\pm^0 + w}\left(\frac{\alpha}{M_\pm^0 + w} + \frac{cM_\pm^0\alpha}{(M_\pm^0 + w)^2} - \frac{cw\alpha}{(M_\pm^0 + w)^2}\right)\\ &= \frac{B_\pm^0 M_\pm^0 \alpha}{(M_\pm^0 + w)^3}(M_\pm^0(c+1) + w(1-c)). \end{aligned} \tag{36}$$

In order to determine the sign of the determinant of the Jacobian at the interior equilibrium $(M_\pm^0, B_\pm^0)$, we consider the following two cases based on the existence of the interior equilibria E_+^0 and E_-^0:

Case 1: If $0 \le c \le 1$, the model (35) has a unique positive equilibrium E_+^0 for $d_m \in (0, \widetilde{d}_{m,0})$ and there is no positive equilibrium if $d_m > \widetilde{d}_{m,0}$.
In this case, for the interior equilibrium E_+^0, the determinant is given by

$$\text{Det} = \frac{B_+^0 M_+^0 \alpha}{(M_+^0 + w)^3}(M_+^0(c+1) + w(1-c)) > 0.$$

Therefore, in this case the interior equilibrium E_+^0 is locally asymptotically stable.

Case 2: If $c > 1$, for $d_m > d_{m,0}^*$, there is no positive equilibrium; for $d_m \in (\widetilde{d}_{m,0}, d_{m,0}^*)$, there are exactly two positive equilibria of the model (35), $E_\pm^0 = (M_\pm^0, B_\pm^0)$; for $d_m \in (0, \widetilde{d}_{m,0}]$, there is only one positive equilibrium $E_+^0 = (M_+^0, B_+^0)$.
In this case,

$$\text{Det} = \frac{B_+^0 M_+^0 \alpha}{(M_+^0 + w)^3}(M_+^0(c+1) + w(1-c)) > 0,$$

and

$$\text{Det} = \frac{B_-^0 M_-^0 \alpha}{(M_-^0 + w)^3}(M_-^0(c+1) + w(1-c)) < 0.$$

since $M_+^0 > \widetilde{M} = \dfrac{w(c-1)}{1+c}$ and $M_-^0 < \widetilde{M} = \dfrac{w(c-1)}{1+c}$.

Based on the above analysis, we have the following theorem which summarizes the local stability of the equilibria of the system (35).

Theorem 4.1 *Recall the bifurcation points $\widetilde{d}_{m,\tau}$ and $d_{m,\tau}^*$ defined as in (33) (with $\tau = 0$). For the ODE system (35), the trivial equilibrium $E_0 = (0, 0)$ is a saddle point*

for all parameters $\alpha, w, d_m > 0$ and $c \geq 0$; and the boundary equilibrium $E_1 = (0, 1)$ is a saddle point if $d_m < \widetilde{d}_{m,0}$, and E_1 is locally asymptotically stable if $d_m > \widetilde{d}_{m,0}$. For the interior equilibria $E^0_\pm = (M^0_\pm, B^0_\pm)$ defined in (34), there are two cases:

1. *If $c > 1$, for $d_m > d^*_{m,0}$, there is no positive equilibrium; for $d_m \in (\widetilde{d}_{m,0}, d^*_{m,0})$, there are two positive equilibria $E^0_\pm$ of the model (35), E^0_+ is locally asymptotically stable and E^0_- is a saddle point; for $d_m \in (0, \widetilde{d}_{m,0}]$, there is only one positive equilibrium E^0_+ which is locally asymptotically stable.*
2. *If $0 \leq c \leq 1$, then for $d_m > \widetilde{d}_{m,0}$, there is no positive equilibrium; for $d_m \in (0, \widetilde{d}_{m,0}]$ the model (35) has only one positive equilibrium E^0_+, which is locally asymptotically stable.*

We remark that (35) is a cooperative system, and all solutions of (35) are bounded, hence when there is only one locally stable equilibrium point, it is indeed globally asymptotically stable from Poincáre–Bendixon Theorem as there is no periodic orbits from the phase portrait; on the other hand, when there are two locally stable equilibria E^0_+ and E_1 when $d_m \in (\widetilde{d}_{m,0}, d^*_{m,0})$, then there is a curve (the stable manifold of E^0_-) in $\mathbb{R}^2_+$ separating the basins of attraction of E^0_+ and E_1. The latter result is a special case of a result of Jiang et al. (2004), see also the survey article of Jiang and Shi (2010). Therefore the global dynamics of the system (35) is completely determined from the bifurcation and local stability result in Theorem 4.1.

For the dynamics of ODE system (35), one can define a basic reproduction number

$$R^0_0 = \frac{\alpha}{w d_m}.$$

Even without eating mistletoe fruits, the bird population grows at a logistic rate. Hence when $R^0_0 \leq 1$, the no-mistletoe equilibrium E_1 is locally asymptotically stable, and when $R^0_0 > 1$, a coexistence equilibrium E^0_+ is locally (indeed globally) asymptotically stable. For small mistletoe-to-bird conversion rate c ($0 \leq c \leq 1$), the basic reproduction number R^0_0 completely determines the asymptotical dynamics, as the global attractor changes from E_1 to E^0_+ as R^0_0 crosses the threshold value 1. For larger values of c ($c > 1$), there is a bistable regime for $R^0_0 < 1$ for which E_1 and E^0_+ both exist and are locally asymptotically stable.

Hence for the ODE system (35), the parameters R^0_0 and c completely determines the long time dynamics of the mistletoe and bird interaction. Note that R^0_0 is determined by the mistletoe fruit hanging rate α, the bird handling time h, and the mistletoe death rate d_m.

4.3 Linearized stability analysis II: effect of delay in non-spatial model

Secondly we examine the stability of constant equilibria in the equation with delay but without the spatial structure (again assuming that the spatial domain Ω is the set of a single point). Then the system (26) is now

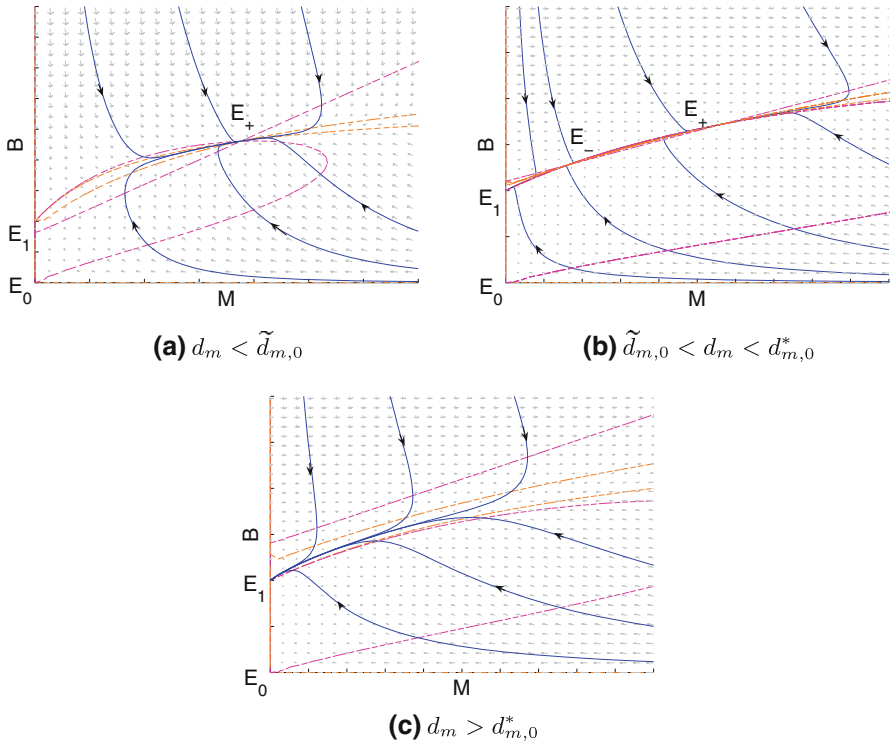

Fig. 3 Phase portraits of model (35) for d_m in different ranges. In **a**, $d_m < \widetilde{d}_{m,0}$, there is one stable interior equilibrium E_+, and E_0 and E_1 are unstable; **b**, $\widetilde{d}_{m,0} < d_m < d^*_{m,0}$, we have bistable dynamics, E_1 and E_+ are locally asymptotically stable and E_0 and E_- are unstable; **c**, $d_m > d^*_{m,0}$, there is no interior equilibrium, E_0 is unstable and E_1 is globally asymptotically stable. Parameter used: $w = 1$, $\alpha = 1$, $c = 2$, and **a** $d_m = 0.8$, **b** $d_m = 1.1$ and **c** $d_m = 1.4$

$$\begin{cases} M' = \dfrac{\alpha e^{-d_i \tau} M(t-\tau) B(t-\tau)}{M(t-\tau) + w} - d_m M, \\ B' = B(1-B) + \dfrac{cMB}{M+w}, \end{cases} \tag{37}$$

where $\tau > 0$ is the time delay. It is easy to see that the equilibria $E_0 = (0, 0)$ and $E^\tau_- = (M^\tau_-, B^\tau_-)$ are all unstable with respect to the dynamics of (37) as they are unstable with respect to (35). The characteristic equation of the linearization of (37) at $E_1 = (0, 1)$ is (Fig. 3)

$$\det \begin{pmatrix} \dfrac{\alpha e^{-d_i \tau}}{w} e^{-\lambda \tau} - d_m - \lambda & 0 \\ \dfrac{c}{w} & -1 - \lambda \end{pmatrix} = 0.$$

So the stability of E_1 is determined by the roots of

$$H(\lambda) := \lambda + d_m - \frac{\alpha e^{-d_i \tau}}{w} e^{-\lambda \tau} = 0. \tag{38}$$

It is straightforward that (38) always has a positive root if $d_m < \widetilde{d}_{m,\tau}$ since $H(0) < 0$ and $H(\infty) > 0$, and exact one zero root with all the other roots having negative real parts if $d_m = \widetilde{d}_{m,\tau}$. Suppose $\pm i\nu$, $(\nu > 0)$, are a pair of pure imaginary roots of (38), we have

$$d_m - \widetilde{d}_{m,\tau} \cos \nu\tau = 0, \quad \text{and} \quad \nu + \widetilde{d}_{m,\tau} \sin \nu\tau = 0.$$

Then $d_m^2 + \nu^2 = \widetilde{d}_{m,\tau}^2$, which implies no roots cross the imaginary axis when $d_m > \widetilde{d}_{m,\tau}$. Therefore, for (37), E_1 is unstable if $d_m < \widetilde{d}_{m,\tau}$ and is locally asymptotically stable if $d_m > \widetilde{d}_{m,\tau}$ for any $\tau > 0$.

It remains to consider the stability of $E_+^\tau = (M_+^\tau, B_+^\tau)$. Here we assume that $\tau > 0$ is fixed. The linearization of system (37) at the equilibrium E_+^τ has solutions with form $\exp(\lambda t)$ whenever λ satisfies

$$\det \begin{pmatrix} \dfrac{wd_m}{M_+^\tau + w} e^{-\lambda\tau} - d_m - \lambda & \dfrac{\alpha e^{-d_i\tau} M_+^\tau}{M_+^\tau + w} e^{-\lambda\tau} \\ \dfrac{cwB_+^\tau}{(M_+^\tau + w)^2} & -B_+^\tau - \lambda \end{pmatrix} = 0.$$

So λ is the root of $G(\cdot, \tau) = 0$ where

$$\begin{aligned} G(\lambda, \tau) := & \left(\frac{wd_m}{M_+^\tau + w} e^{-\lambda\tau} - d_m - \lambda \right) \left(-B_+^\tau - \lambda \right) \\ & - \left(\frac{\alpha e^{-d_i\tau} M_+^\tau}{M_+^\tau + w} \right) \left(\frac{cwB_+^\tau}{(M_+^\tau + w)^2} \right) e^{-\lambda\tau}. \end{aligned}$$

Since the system is cooperative, then the stability of E_+^τ is determined by its stability module $\lambda_s(\tau)$ defined as

$$\lambda_s(\tau) = \max\{\mathcal{R}e(\lambda) : G(\lambda, \tau) = 0\}.$$

E_+^τ is stable if $\lambda_s(\tau) < 0$ and unstable otherwise. From Theorem 5.1 of Smith (1995), p. 92 or Theorem 3.2 of Wu (1992), $\lambda_s(\tau)$ is a root of $G(\cdot, \tau) = 0$ of algebraic multiplicity 1, and for any other root λ of $G(\cdot, \tau) = 0$ then $\mathcal{R}e(\lambda) < \lambda_s(\tau)$.

Notice that for any fixed $\tau_0 > 0$,

$$G(0, \tau_0) = e^{-d_i\tau_0} \frac{B_+^{\tau_0} M_+^{\tau_0} \alpha}{(M_+^{\tau_0} + w)^3} (M_+^{\tau_0}(c+1) + w(1-c)),$$

which is the determinant of the Jacobian matrix evaluated at E_+^τ when the delay is zero. By the results in Sect. 4.2, we have $G(0, \tau_0) > 0$. Since $\lambda_s(\tau)$ is real-valued, hence we can restrict the definition of F to $\mathbb{R} \times \mathbb{R}^+$. If we can prove that $\dfrac{\partial G(\lambda, \tau_0)}{\partial \lambda} > 0$ for all positive λ, we gain that all the real roots of $G(\lambda, \tau_0) = 0$ are negative.

By straightforward calculation, we have

$$\frac{\partial G(\lambda,\tau_0)}{\partial\lambda} = (\lambda + B_+^{\tau_0})(1 + \frac{w\tau_0 d_m e^{-\lambda\tau_0}}{M_+^{\tau_0}+w}) + \lambda + d_m - \frac{w d_m e^{-\lambda\tau_0}}{M_+^{\tau_0}+w} + \left(\frac{\alpha e^{-d_i\tau_0} M_+^{\tau_0}}{M_+^{\tau_0}+w}\right)\left(\frac{cwB_+^{\tau_0}}{(M_+^{\tau_0}+w)^2}\right) e^{-\lambda\tau_0} > 0,$$

for all positive λ. Therefore we have $\frac{\partial G(\lambda,\tau_0)}{\partial\lambda} > 0$ for all positive λ, which implies that $\lambda_s(\tau_0)$ must be negative. Hence we prove that the equilibrium E_+^τ is locally stable for any delay $\tau > 0$.

We summarize the dynamical behavior of the system (37) as follows, which is similar to the case of $\tau = 0$ as in Theorem 4.1:

Theorem 4.2 *Recall the bifurcation points $\widetilde{d}_{m,\tau}$ and $d^*_{m,\tau}$ defined as in (33). For the system (37), the trivial equilibrium $E_0 = (0,0)$ is a saddle point for all parameters $\alpha, c, w, d_m > 0$; and the boundary equilibrium $E_1 = (0,1)$ is a saddle point if $d_m < \widetilde{d}_{m,\tau}$, and E_1 is locally asymptotically stable if $d_m > \widetilde{d}_{m,\tau}$. For the interior equilibria $E_\pm^\tau = (M_\pm^\tau, B_\pm^\tau)$ defined in (34), there are two cases:*

1. *If $c > 1$, for $d_m > d^*_{m,\tau}$, there is no positive equilibrium; for $d_m \in (\widetilde{d}_{m,\tau}, d^*_{m,\tau})$, there are two positive equilibria $E_\pm^0$ of the model (37), E_+^τ is locally asymptotically stable and E_-^τ is a saddle point; for $d_m \in (0, \widetilde{d}_{m,\tau}]$, there is only one positive equilibrium E_+^τ which is locally asymptotically stable.*
2. *If $0 \le c \le 1$, then for $d_m > \widetilde{d}_{m,\tau}$, there is no positive equilibrium; for $d_m \in (0, \widetilde{d}_{m,\tau}]$ the model (37) has only one positive equilibrium E_+^τ, which is locally asymptotically stable.*

Comparing the dynamics of delayed system (37) with the one of ODE system (35), we notice that the time-delay does not cause any qualitative change to the bifurcation diagram (see Figs. 1, 2). The shape of the equilibrium bifurcation diagrams for $\tau > 0$ and $\tau = 0$ are same, but there is a shift of the bifurcation points as

$$d^*_{m,\tau} = e^{-d_i\tau} d^*_{m,0}, \quad \text{and} \quad \widetilde{d}_{m,\tau} = e^{-d_i\tau}\widetilde{d}_{m,0}.$$

We can also observe that the basic reproduction number in the time-delayed case can be defined as

$$R_0^\tau = \frac{\alpha}{w d_m e^{d_i\tau}} = e^{-d_i\tau} R_0^0.$$

Hence the time-delay decreases the basic reproduction number of the system, and the growth of the mistletoe is more difficult with the delay.

The impact of the time-delay to the dynamics can be clearly observed from time plots with $\tau = 0$ and $\tau = 1$ in Figs. 4, 5, 6, 7, 8: (all plots have same initial conditions for $\tau = 0$ and $\tau = 1$)

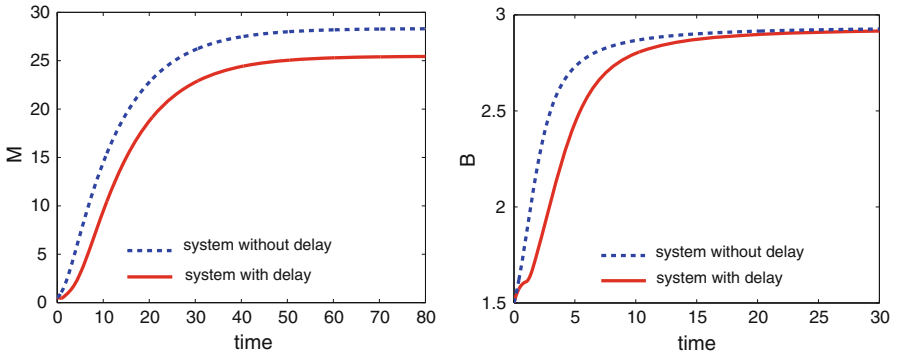

Fig. 4 Time plots of system (35) (*dashed blue*) and (37) (*solid red*) with $w = 1, \alpha = 1, c = 2, d_m = 0.1, d_i = 0.1$ and $\tau = 1$. Both system have a unique positive equilibrium E_+. Time delay could reduce the final population of mistletoes and birds without affecting the stability of E_+

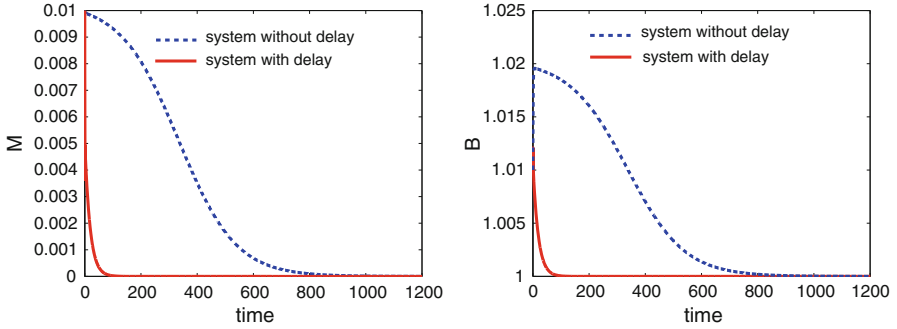

Fig. 5 Time plots of system (35) (*dashed blue*) and (37) (*solid red*) with $w = 1, \alpha = 1, c = 2, d_m = 1.01, d_i = 0.1$ and $\tau = 1$. Both systems have two positive equilibria E_+ and E_-. Initial values close to E_1 produce solutions that tends to E_1 for both systems, but the solution of the time-delay system converges to E_1 much faster

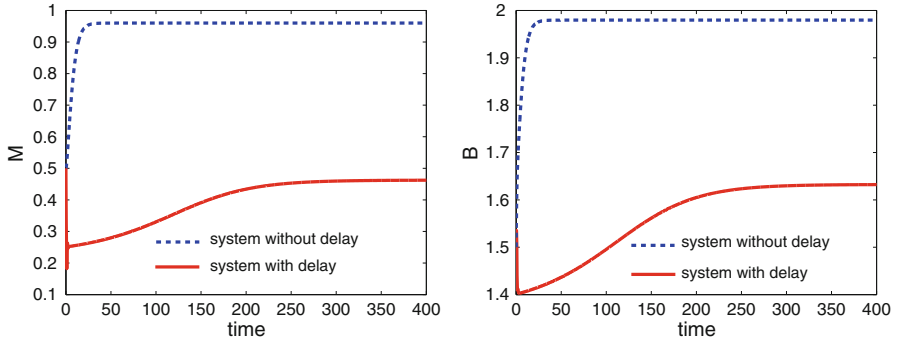

Fig. 6 Time plots of system (35) (*dashed blue*) and (37) (*solid red*) with $w = 1, \alpha = 1, c = 2, d_m = 1.01, d_i = 0.1$ and $\tau = 1$. Both systems have two positive equilibria E_+ and E_-. Initial values close to E_+ produce solutions that tends to E_+ for both systems, but the time-delay slows down the convergence rate

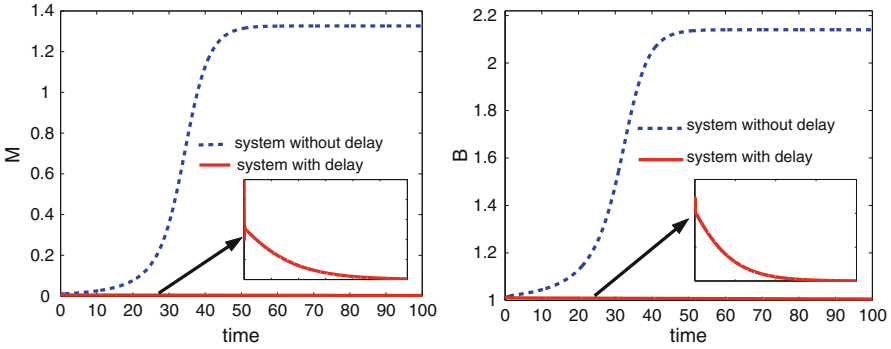

Fig. 7 Time plots of system (35) (*dashed blue*) and (37) (*solid red*) with $w = 1, \alpha = 1, c = 2, d_m = 0.92, d_i = 0.1$ and $\tau = 1$. Here E_+^0 is the globally stable positive equilibrium for (35), while the dynamics of (37) is bistable

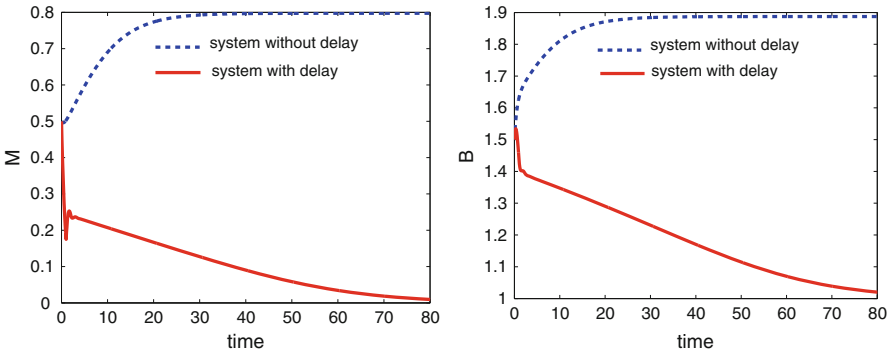

Fig. 8 Time plots of system (35) (*dashed blue*) and (37) (*solid red*) with $w = 1, \alpha = 1, c = 2, d_m = 1.05, d_i = 0.1$ and $\tau = 1$. Here the dynamics of (35) is bistable stable, while for (37) E_1 is globally asymptotically stable

1. The stable positive equilibrium E_+^τ for the time-delayed system is smaller than the one E_+^0 without delay, and it takes longer time to converge to E_+^τ with the same initial values (see Figs. 4, 6);
2. When solutions converge to the mistletoe-extinction equilibrium E_1, the convergence for the time-delayed system is faster than the one without delay (see Fig. 5);
3. It is possible that for some d_m value, the time-delayed system and no-delay system are both bistable (see Figs. 5, 6) as the bistability intervals $(\widetilde{d}_{m,\tau}, d^*_{m,\tau})$ and $(\widetilde{d}_{m,0}, d^*_{m,0})$ have overlap part for small $\tau > 0$. However for d_m value not in this overlap part, the dynamical behavior for certain initial values can be drastically different. For example, when the dynamics of delayed system is bistable and the one of no-delay system is monostable with E_+^0, then a small initial value can lead to extinction in delayed system while the same initial value can eventually stabilize at positive equilibrium (see Fig. 7). On the other hand, the dynamics of no-delay system can be bistable and the one for delayed system is monostable with E_1, then

a large initial value can lead to persistence for the no-delay system but the same initial value still leads to extinction for the delayed system (see Fig. 8).

4.4 Linearized stability analysis III: spatial model

Lastly we study the spatial model (26) and examine the stability of the constant equilibria in the dynamics with both diffusion and delay effect but not the nonlocal effect. We consider boundary value problem:

$$\begin{cases} \dfrac{\partial M}{\partial t} = \alpha e^{-d_i\tau}\dfrac{M(t-\tau,x)}{M(t-\tau,x)+w}B(t-\tau,x) - d_m M, & x\in\overline{\Omega}, t>0, \\ \dfrac{\partial B}{\partial t} = D\Delta B - \beta\nabla(B\nabla M) + B(1-B) + \dfrac{cMB}{M+w}, & x\in\Omega, t>0, \\ M(t,x) = M_0(t,x),\ B(0,x) = B_0(x), & x\in\Omega, -\tau\le t\le 0, \\ [D\nabla B(t,x) - \beta B(t,x)\nabla M(t,x)]\cdot n(x) = 0, & x\in\partial\Omega. \end{cases} \tag{39}$$

It is obvious that the existence result on the equilibria in Theorem 4.2 is also applicable to (39). Let (M^*, B^*) be any constant equilibrium of (39). The linearization of (39) at (M^*, B^*) is

$$\begin{cases} \dfrac{\partial \Phi}{\partial t} = \dfrac{\alpha e^{-d_i\tau} w B^*}{(M^*+w)^2}\Phi_\tau - d_m\Phi + \dfrac{\alpha e^{-d_i\tau}M^*}{M^*+w}\Psi_\tau, & x\in\overline{\Omega}, t>0, \\ \dfrac{\partial \Psi}{\partial t} = D\triangle\Psi - \beta B^*\triangle\Phi + \dfrac{cwB^*}{(M^*+w)^2}\Phi + (1-2B^* + \dfrac{cM^*}{M^*+w})\Psi, & x\in\Omega, t>0, \\ [D\nabla\Psi - \beta B^*\nabla\Phi]\cdot n = 0, & x\in\partial\Omega, t>0, \end{cases} \tag{40}$$

where $\Phi_\tau = \Phi(t-\tau,x)$ and $\Psi_\tau = \Psi(t-\tau,x)$. Substituting $\Phi(t,x) = e^{\lambda t}\phi(x)$ and $\Psi(t,x) = e^{\lambda t}\psi(x)$ into (40) gives

$$\begin{cases} \lambda\phi = \dfrac{\alpha e^{-d_i\tau} w B^*}{(M^*+w)^2}e^{-\lambda\tau}\phi - d_m\phi + \dfrac{\alpha e^{-d_i\tau}M^*}{M^*+w}e^{-\lambda\tau}\psi, & x\in\overline{\Omega}, \\ \lambda\psi = D\triangle\psi - \beta B^*\triangle\phi + \dfrac{cwB^*}{(M^*+w)^2}\phi + (1-2B^* + \dfrac{cM^*}{M^*+w})\psi, & x\in\Omega, \\ [D\nabla\psi - \beta B^*\nabla\phi]\cdot n = 0, & x\in\partial\Omega. \end{cases} \tag{41}$$

From the first equation of (41), ϕ and ψ are linearly dependent. Hence both of ϕ and ψ satisfy the homogeneous Neumann boundary condition, and from the second equation of (41), $(\phi,\psi) = (\alpha,\beta)y$ for some eigenfunction y of $-\Delta$ on Ω with Neumann boundary condition. Let $\{\mu_n\}$ be the sequence of eigenvalues of $-\Delta$ on Ω with Neumann boundary condition, such that $0 = \mu_0 < \mu_1 \le \mu_2 \le \cdots$, and let $y_n(x)$ be the corresponding eigenfunctions, $n = 0, 1, \ldots$. Then by using Fourier expansion,

there exist $n \in \mathbb{N} \cup \{0\}$, and $\alpha_n, \beta_n \in \mathbb{R}$ such that $(\phi, \psi) = (\alpha_n, \beta_n) y_n$, which leads to the following transcendental characteristic equation

$$\det \begin{pmatrix} \dfrac{\alpha e^{-d_i \tau} w B^*}{(M^* + w)^2} e^{-\lambda\tau} - d_m - \lambda & \dfrac{\alpha e^{-d_i \tau} M^*}{M^* + w} e^{-\lambda\tau} \\ \dfrac{cwB^*}{(M^* + w)^2} + \beta B^* \mu_n & 1 - 2B^* + \dfrac{cM^*}{M^* + w} - D\mu_n - \lambda \end{pmatrix} = 0. \quad (42)$$

When $(M^*, B^*) = (0, 0)$, (42) becomes

$$(\lambda + d_m)(\lambda + D\mu_n - 1) = 0,$$

which implies $(0, 0)$ is always unstable. When $(M^*, B^*) = (0, 1)$, (42) turns into

$$\left(\lambda + d_m - \frac{\alpha e^{-d_i \tau}}{w} e^{-\lambda\tau}\right)(\lambda + D\mu_n + 1) = 0,$$

of which all the roots have negative real parts if $d_m > \widetilde{d}_{m,\tau}$, and it has one positive root if $d_m < \widetilde{d}_{m,\tau}$. At (M_+^τ, B_+^τ), (42) is equivalent to

$$G_n(\lambda, \tau) := \lambda^2 + T_n(\tau)\lambda + U_n(\tau) - (V_n(\tau)\lambda + W_n(\tau))e^{-\lambda\tau} = 0, \quad (43)$$

where

$$T_n(\tau) = d_m + B_+^\tau + D\mu_n, \quad U_n(\tau) = d_m(B_+^\tau + D\mu_n), \quad V_n(\tau) = \frac{d_m w}{M_+^\tau + w},$$
$$W_n(\tau) = (B_+^\tau + D\mu_n)\frac{d_m w}{M_+^\tau + w} + d_m M_+^\tau \left(\frac{cw}{(M_+^\tau + w)^2} + \mu_n \beta\right).$$

For any fixed $\tau_0 > 0$, if $\beta < \dfrac{D}{M_+^0 + w}$, we have

$$\begin{aligned} &G_n(0, \tau_0) \\ &= U_n(\tau_0) - W_n(\tau_0) \\ &= d_m B_+^{\tau_0} - \frac{cw d_m M_+^{\tau_0}}{(M_+^{\tau_0} + w)^2} - \frac{d_m w B_+^{\tau_0}}{M_+^{\tau_0} + w} + d_m \mu_n \left(D - \beta M_+^{\tau_0} - \frac{Dw}{M_+^{\tau_0} + w}\right) \\ &= \frac{d_m M_+^{\tau_0}}{(M_+^{\tau_0} + w)^2}[(c+1)M_+^{\tau_0} + (1-c)w] + d_m \mu_n M_+^{\tau_0} \left(\frac{D}{M_+^{\tau_0} + w} - \beta\right) > 0, \end{aligned} \quad (44)$$

for $n = 0, 1, \ldots$, since $M_+^0 > M_+^{\tau_0}$ and $M_+^{\tau_0} > \widetilde{M} = \dfrac{(c-1)w}{1+c}$ if $c > 1$. Also

$$\frac{\partial G_n(\lambda, \tau_0)}{\partial \lambda} = 2\lambda + T_n(\tau_0) - V_n(\tau_0)e^{-\lambda\tau_0} + \tau_0(V_n(\tau_0)\lambda + W_n(\tau_0))e^{-\lambda\tau_0} > 0, \quad (45)$$

for all positive λ. Combining (44) and (45), we conclude that the stability module $\lambda_s^n(\tau) = \max\{\mathcal{R}e(\lambda) : G_n(\lambda, \tau) = 0\}$, which is a root of $G_n(\lambda, \tau) = 0$ of algebraic multiplicity one from Theorem 5.1 in Smith (1995), ia negative for $n = 0, 1, \ldots$. Similar arguments as the above ones indicate that the constant equilibrium (M_-^τ, B_-^τ), whenever exists, is unstable since the corresponding characteristic equation has a positive root for all $\tau \geq 0$ when $n = 0$. Summarizing the above analysis, we have the following conclusion.

Theorem 4.3 *Recall the bifurcation points $\widetilde{d}_{m,\tau}$ and $d^*_{m,\tau}$ defined as in (33). For the system (39), the trivial equilibrium $E_0 = (0, 0)$ is unstable for all parameters; and the boundary equilibrium $E_1 = (0, 1)$ is unstable if $d_m < \widetilde{d}_{m,\tau}$, and is locally asymptotically stable if $d_m > \widetilde{d}_{m,\tau}$. The existence of interior equilibria $E_\pm^\tau = (M_\pm^\tau, B_\pm^\tau)$ defined in (34) follows from Theorem 4.2. Furthermore, E_-^τ is unstable and E_+^τ is locally asymptotically stable if $\beta < \dfrac{D}{M_+^0 + w}$.*

Comparing the results in Theorem 4.3 with the ones in Theorem 4.2, the stability of constant equilibrium E_+^τ still holds for system (39) with the additional effect of diffusion but not chemotaxis ($\beta = 0$). However with a large chemotactic coefficient $\beta > 0$, E_+^τ may lose the stability.

5 Bifurcation analysis of the model with chemotactic and nonlocal effect

If the dispersal mapping is not an identity map as in Sect. 4, then in general the system (25) does not possess constant equilibria besides $E_0 = (0, 0)$ and $E_1 = (1, 0)$. In this section we consider the existence of non-constant equilibria of (25) under more general assumptions on the dispersal operator $K[u]$. For this general case, the existence of solutions to the dynamical Eq. (9) when $\beta = 0$ has been shown in Sect. 3, and indeed numerical simulations for any $\beta \geq 0$ (see Sect. 6) suggest that most dynamical solutions converge to equilibrium solutions. Hence the existence and profile of non-constant equilibria is critical for the understanding of the dynamics.

For the results in this section, besides $(K1)$ and $(K2)$, we also assume that the dispersal operator $K : C(\overline{\Omega}) \to C(\overline{\Omega})$ satisfies

$(K3)$ $K : C(\overline{\Omega}) \to C(\overline{\Omega})$ is compact, and K is strongly positive, that is, for any $u \in C(\overline{\Omega})$ and $u \geq 0$, $K[u](x) > 0$ for $x \in \overline{\Omega}$.

We notice that the identity mapping $K[u] = u$ considered in Sect. 4 does not satisfy $(K3)$, but the integral operator defined in $(H2)$ satisfies $(K3)$ if the kernel function $k(x, y) > 0$ for $(x, y) \in \overline{\Omega} \times \overline{\Omega}$. The main consequence of the assumption $(K3)$ is the renown Krein–Rutman Theorem which asserts the existence of a principal eigenvalue with a positive eigenvector.

In this section, we conduct a bifurcation analysis of the non-constant equilibria of the model (25) with $\beta \geq 0$. That is

$$\begin{cases} \alpha e^{-d_i\tau} K\left[\dfrac{MB}{M+w}\right](x) - d_m M(x) = 0, & x \in \overline{\Omega}, \\ D\Delta B(x) - \beta\nabla(B(x)\nabla M(x)) + B(x)(1-B(x)) + cK\left[\dfrac{MB}{M+w}\right](x) = 0, & x \in \Omega, \\ [D\nabla B(x) - \beta B(x)\nabla M(x)]\cdot n(x) = 0, & x \in \partial\Omega. \end{cases} \tag{46}$$

Using d_m as a bifurcation parameter, the equilibrium problem (46) can be written in the following abstract form:

$$F(d_m, M, B) = 0, \tag{47}$$

where $F : \mathbb{R} \times W^{2,p}(\Omega) \times W^{2,p}(\Omega) \to W^{2,p}(\Omega) \times L^p(\Omega) \times W^{1,p}(\partial\Omega)$ is defined by

$$F(d_m, M, B) = \begin{pmatrix} \alpha e^{-d_i\tau} K\left[\dfrac{MB}{M+w}\right] - d_m M \\ D\Delta B - \beta\nabla(B\nabla M) + B(1-B) + cK\left[\dfrac{MB}{M+w}\right] \\ (D\nabla B - \beta B\nabla M)\cdot n \end{pmatrix}. \tag{48}$$

Here $p > n$ (where n is the spatial dimension) and $W^{k,p}(\Omega)$, $W^{k,p}(\partial\Omega)$ are the Sobolev spaces. Recall that under the assumption $p > n$, $W^{2,p}(\Omega)$ is compactly embedded in $C(\overline{\Omega})$. Solutions of (47) are weak solutions of the equilibrium equation of (9). From the smoothness of nonlinearities in the system (9), these weak solutions in the Sobolev spaces are indeed classical solutions in $C(\overline{\Omega}) \times C^{2,\gamma}(\overline{\Omega})$ from the elliptic estimates.

Suppose that $(\hat{M}, \hat{B})$ is an equilibrium of (46). Then the stability of this equilibrium is determined by the following P-eigenvalue problem (see Crandall and Rabinowitz 1973):

$$F_{(M,B)}(d_m, \hat{M}, \hat{B})[(\phi, \psi)] = \lambda P[(\phi, \psi)],$$

where the linear mapping $P : W^{2,p}(\Omega)\times W^{2,p}(\Omega) \to W^{2,p}(\Omega)\times L^p(\Omega)\times W^{1,p}(\partial\Omega)$ is defined by $P[(\phi, \psi)] = (\phi, \psi, 0)$. Again the model (46) has two trivial solutions $E_0 = (0, 0)$ and $E_1 = (0, 1)$ for any $d_m > 0$. We consider the bifurcation of non-trivial solutions to (47) from the line of trivial solutions $\{(d_m, 0, 1) : d_m > 0\}$. The linearization of F at the boundary equilibrium $E_1 = (0, 1)$ is

$$F_{(M,B)}(d_m, 0, 1)[\phi, \psi] = \begin{pmatrix} \dfrac{\alpha e^{-d_i\tau}}{w} K[\phi] - d_m\phi \\ D\Delta\psi - \psi + \dfrac{c}{w}K[\phi] - \beta\Delta\phi \\ (D\nabla\psi - \beta\nabla\phi)\cdot n \end{pmatrix}.$$

Therefore, 0 is a simple eigenvalue of $F_{(M,B)}(d_m, 0, 1)$ if and only if

$$\begin{cases} K[\phi] = \dfrac{d_m w}{\alpha e^{-d_i \tau}}\phi, & x \in \overline{\Omega}, \\ -D\Delta\psi + \psi = \dfrac{c}{w}K[\phi] - \beta\Delta\phi, & x \in \Omega, \\ \dfrac{\partial\psi}{\partial n} = \dfrac{\beta}{D}\dfrac{\partial\phi}{\partial n}, & x \in \partial\Omega. \end{cases} \tag{49}$$

has a unique nonzero solution up to a constant multiple. From the compactness assumption in $(K3)$, it follows from well-known results for compact operators, $K : C(\overline{\Omega}) \to C(\overline{\Omega})$ possesses a sequence of eigenvalues $\{\lambda_i\}$ such that $\lambda_i \in \mathbb{R}$,

$$0 \le \cdots \le |\lambda_3| \le |\lambda_2| \le |\lambda_1|, \tag{50}$$

and the only possible limit point of $\{\lambda_i\}$ is zero. Moreover, since K is strongly positive, then from Krein–Rutman theorem (see Chang 2005), we have ft$\lambda_1 > 0$ with its corresponding function $\phi_1(x) > 0$. In the following we normalize ϕ_1 so that $\max_{x\in\overline{\Omega}} \phi_1(x) = 1$, and we also assume that

$(K4)$ $\phi_1 \in W^{2,p}(\Omega)$ for any $p > n$.

Again we remark that for the integral operators satisfying $(H2)$, the assumption $(K4)$ can be easily verified.

Now we define a new bifurcation point

$$\widetilde{d}^k_{m,\tau} := \widetilde{d}_{m,\tau}\lambda_1 = \frac{\alpha}{w}e^{-d_i\tau}\lambda_1, \tag{51}$$

and let ψ_1 be the unique solution of

$$\begin{cases} -D\Delta\psi + \psi = \dfrac{c\widetilde{d}^k_{m,\tau}}{\alpha e^{-d_i\tau}}\phi_1 - \beta\Delta\phi_1, & x \in \Omega, \\ \dfrac{\partial\psi}{\partial n} = \dfrac{\beta}{D}\dfrac{\partial\phi_1}{\partial n}, & x \in \partial\Omega. \end{cases} \tag{52}$$

Then when $d_m = \widetilde{d}^k_{m,\tau}$, (49) is solvable thus a bifurcation occurs at $d_m = \widetilde{d}^k_{m,\tau}$. Indeed by using the celebrated bifurcation from simple eigenvalue theorem in Crandall and Rabinowitz (1971) and also the global bifurcation theory in Rabinowitz (1971), we arrive at the following bifurcation picture:

Theorem 5.1 *Assume that $\beta \ge 0$, and the dispersal mapping K satisfies (K1)–(K4). Then there is a smooth curve Γ^k_τ of positive equilibrium solutions of (9) bifurcating from the line of trivial solutions $\{(d_m, 0, 1) : d_m > 0\}$ at $d_m = \widetilde{d}^k_{m,\tau}$, and Γ^k_τ is contained in a global branch $\mathcal{C}^k_\tau$ of positive equilibrium solutions of (9). Moreover*

1. *Near $(d_m, M, B) = (\widetilde{d}^k_{m,\tau}, 0, 1)$, $\Gamma^k_\tau = \{(d_m(s), M(s,x), B(s,x)) : s \in (0,\epsilon)\}$, where $M(s,x) = s\phi_1(x) + s\Psi_1(s,x)$, $B(s,x) = 1 + s\psi_1(x) + s\Psi_2(s,x)$, ϕ_1 is the principal eigenfunction of K, and ψ_1 is defined as in (52); $d_m(s)$, $\Psi_1(s,\cdot)$*

and $\Psi_2(s,\cdot)$ *are smooth functions defined for* $s \in (0,\epsilon)$ *such that* $\Psi_1(0,\cdot) = \Psi_2(0,\cdot) = 0$, $d_m(0) = \widetilde{d}^k_{m,\tau}$, *and*

$$d_m'(0) = \frac{\alpha e^{-d_i\tau}\int_\Omega K[-\phi_1^2(\cdot) + w\phi_1(\cdot)\psi_1(\cdot)](x)\phi_1(x)dx}{w^2\int_\Omega \phi_1^2(x)dx}. \tag{53}$$

2. *For* $s \in (0,\epsilon)$, *the bifurcating solution* $(d_m(s), M(s,\cdot), B(s,\cdot))$ *is locally asymptotically stable if* $d_m'(0) < 0$, *and it is unstable if* $d_m'(0) > 0$.
3. *Additioanlly assume that* $\beta = 0$. *Let* $\mathbf{proj}_{d_m}\mathcal{C}^k_\tau$ *be the projection of the global branch* $\mathcal{C}^k_\tau$ *onto* d_m*-axis. Then* $\mathbf{proj}_{d_m}\mathcal{C}^k_\tau = (0, d^{*,k}_{m,\tau}]$, *where* $d^{*,k}_{m,\tau}$ *satisfies*

$$\frac{\alpha}{w}e^{-d_i\tau}\lambda_1 \equiv \widetilde{d}^k_{m,\tau} \le d^{*,k}_{m,\tau} \le \frac{\alpha e^{-d_i\tau}}{w}A_2A_4\max\{1,|\Omega|\}, \tag{54}$$

where A_2 *and* A_4 *are defined in* $(K2)$ *and* (20).

Proof Here for a linear operator L, we use $N(L)$ as the null space of L and $R(L)$ as the range space of L. It has been shown that (ϕ_1,ψ_1) is the unique (normalized) solution to (49) when $d_m = \widetilde{d}^k_{m,\tau}$. Then we have $(\phi_1,\psi_1) \in N(F_{(M,B)}(\widetilde{d}^k_{m,\tau},0,1))$ and $\dim N(F_{(M,B)}(\widetilde{d}^k_{m,\tau},0,1)) = 1$. Suppose that $(h,g,q) \in R(F_{(M,B)}(\widetilde{d}^k_{m,\tau},0,1))$, *i.e.* there exists $(\varphi,\theta) \in W^{2,p}(\Omega)\times W^{2,p}(\Omega)$ such that

$$\begin{cases} K[\varphi] - \dfrac{\widetilde{d}^k_{m,\tau}w}{\alpha e^{-d_i\tau}}\varphi = h, & x\in\overline{\Omega},\\ D\Delta\theta - \theta + \dfrac{c}{w}K[\varphi] - \beta\Delta\varphi = g, & x\in\Omega,\\ D\dfrac{\partial\theta}{\partial n} - \beta\dfrac{\partial\varphi}{\partial n} = q, & x\in\partial\Omega. \end{cases} \tag{55}$$

The first equation of (55) is solvable if and only if $\langle h,\phi_1\rangle = 0$, and given any φ, g and q, the second and third equations in (55) are always uniquely solvable. Hence $R(F_{(M,B)}(\widetilde{d}^k_{m,\tau},0,1)) = span\{(\phi_1,0,0)\}^\perp$. Finally since $F_{d_m(M,B)}(\widetilde{d}^k_{m,\tau},0,1)[\phi_1,\psi_1] = (-\phi_1,0,0)$, and $\langle -\phi_1,\phi_1\rangle \neq 0$, we know that

$$F_{d_m(M,B)}(\widetilde{d}^k_{m,\tau},0,1)[\phi_1,\psi_1] \notin R(F_{(M,B)}(\widetilde{d}^k_{m,\tau},0,1)).$$

Now by using the local bifurcation theorem in Crandall and Rabinowitz (1971), there exists an open interval $I = (-\epsilon,\epsilon)$ and C^1 functions

$$d_m(s): I\to\mathbb{R}, \quad \text{and} \quad \Psi(s) = (\Psi_1(s,\cdot),\Psi_2(s,\cdot)) : I \to Z,$$

where Z is any complement of $span\{(\phi_1,\psi_1)\}$, such that $d_m(0) = \widetilde{d}^k_{m,\tau}$, $\Psi(0) = (0,0)$, and if $(M(s),B(s)) = (0,1) + s(\phi_1,\psi_1) + s\Psi(s)$ for $s \in I$, then $F(d_m(s),M(s),B(s)) = 0$. Hence a curve of nontrivial solutions $\{(d_m(s),M(s),B(s)) : |s| < \epsilon\}$ of (47) emerges from the bifurcation point $(\widetilde{d}^k_{m,\tau},0,1)$. Moreover, let

l be the linear functional satisfying $N(l) = R(F_{(M,B)}(\widetilde{d}^k_{m,\tau}, 0, 1))$, then from Crandall and Rabinowitz (1971), we have

$$\begin{aligned} d'_m(0) &= -\frac{\langle l,\, F_{(M,B)(M,B)}(\widetilde{d}^k_{m,\tau}, 0, 1)[(\phi_1, \psi_1)(\phi_1, \psi_1)]\rangle}{2\langle l,\, F_{d_m(M,B)}(\widetilde{d}^k_{m,\tau}, 0, 1)[(\phi_1, \psi_1)]\rangle} \\ &= \frac{\alpha e^{-d_i\tau}\int_\Omega K\left[-\frac{2}{w^2}\phi_1^2(\cdot) + \frac{2}{w}\phi_1(\cdot)\psi_1(\cdot)\right](x)\phi_1(x)dx}{2\int_\Omega \phi_1^2(x)dx} \\ &= \frac{\alpha e^{-d_i\tau}\int_\Omega K[-\phi_1^2(\cdot) + w\phi_1(\cdot)\psi_1(\cdot)](x)\phi_1(x)dx}{w^2\int_\Omega \phi_1^2(x)dx} \end{aligned} \tag{56}$$

By using Corollary 1.13 in Crandall and Rabinowitz (1973), we know that there exist continuously differentiable functions $\gamma : (\widetilde{d}^k_{m,\tau} - \varepsilon, \widetilde{d}^k_{m,\tau} + \varepsilon) \to \mathbb{R}$, $\mu : I \to \mathbb{R}$, $u : (\widetilde{d}^k_{m,\tau} - \varepsilon, \widetilde{d}^k_{m,\tau} + \varepsilon) \to L^p(\Omega) \times L^p(\Omega)$ and $v : I \to L^p(\Omega) \times L^p(\Omega)$ such that

$$\begin{aligned} F_{(M,B)}(d_m, 0, 1)[u(d_m)] &= \gamma(d_m)P[u(d_m)], \\ F_{(M,B)}(d_m(s), M(s), B(s))[v(s)] &= \mu(s)P[v(s)], \end{aligned} \tag{57}$$

and

$$\gamma(\widetilde{d}^k_{m,\tau}) = \mu(0) = 0, \quad u(\widetilde{d}^k_{m,\tau}) = v(0) = (\phi_1, \psi_1).$$

The stability of bifurcating equilibrium solutions is determined by the sign of $\mu(s)$. It is straightforward that the P-eigenvalues of $F_{(M,B)}$ at $E_1 = (0, 1)$, denoted by γ_j, $j = 1, 2, \cdots$, are given by

$$\gamma_j = \frac{\alpha e^{-d_i\tau}}{w}\lambda_j - d_m < \frac{\alpha e^{-d_i\tau}}{w}\lambda_1 - d_m \le 0,$$

which implies that $E_1 = (0, 1)$ is locally asymptotically stable if $d_m > \widetilde{d}^k_{m,\tau}$. On the other hand

$$\gamma_1 = \frac{\alpha e^{-d_i\tau}}{w}\lambda_1 - d_m > 0,$$

when $0 < d_m < \widetilde{d}^k_{m,\tau}$, then we know that $E_1 = (0, 1)$ is unstable if $0 < d_m < \widetilde{d}^k_{m,\tau}$. Since $u(\widetilde{d}^k_{m,\tau}) = v(0)$ is positive, then $(M(s), B(s))$ is locally asymptotically stable if $\mu(s) < 0$ and it is unstable if $\mu(s) > 0$. From the first equation of (57), we have

$$\frac{\alpha e^{-d_i\tau}}{w}K[u_1(d_m)] - d_m u_1(d_m) = \gamma(d_m)u_1(d_m),$$

where $u(d_m) = (u_1(d_m), u_2(d_m))$, which implies

$$\lambda_1 \alpha e^{-d_i \tau} = w(d_m + \gamma(d_m)). \tag{58}$$

By differentiating (58) in d_m, we obtain that $\gamma'(\widetilde{d}^k_{m,\tau}) < 0$. Then by using Theorem 1.16 in Crandall and Rabinowitz (1973), we know that the functions $\mu(s)$ and $sd'_m(s)$ have the same sign near $s = 0$ whenever $\mu(s) \neq 0$. If $d'_m(0) > 0$, then $d'_m(s) > 0$ for small s due to the continuity of $d'_m(s)$. Therefore $\mu(s) < 0$ if $d'_m(0) < 0$ and $\mu(s) > 0$ if $d'_m(0) > 0$, which implies the stated stability result.

To apply the global bifurcation theorem in Shi and Wang (2009), we first show that the linearized operator $F_{(M,B)}$ is a Fredholm operator for any $(d_m, M, B) \in \mathbb{R}^+ \times W^{2,p}(\Omega) \times W^{2,p}(\Omega)$. For that purpose we write $F(d_m, M, B) = F_1(d_m, M, B) + F_2(M, B)$, where

$$F_1(d_m, M, B) = \begin{pmatrix} -d_m M \\ D\Delta B - \beta \nabla(B \nabla M) + B(1 - B) \\ (D\nabla B - \beta B \nabla M) \cdot n \end{pmatrix},$$

and

$$F_2(M, B) = \begin{pmatrix} \alpha e^{-d_i \tau} K\left[\dfrac{MB}{M + w}\right] \\ cK\left[\dfrac{MB}{M + w}\right] \\ 0 \end{pmatrix}.$$

It is standard to verify that the linearization $(F_1)_{(M,B)}$ of F_1 at any (d_m, M, B) is Fredholm as $N((F_1)_{(M,B)})$ is finite dimensional, and $R((F_1)_{(M,B)})$ has a finite codimension. And the linearization $(F_2)_{(M,B)}$ of F_2 at any (d_m, M, B) is compact from $(K3)$. Therefore $F_{(M,B)}$ is Fredholm as it is a compact perturbation of a Fredholm operator (see Kato 1995 page 238 Theorem 5.26). Consequently the existence of a global branch $\mathcal{C}^k_\tau$ containing Γ^k_τ follows from Theorem 4.3 of Shi and Wang (2009).

Finally we assume that $\beta = 0$. One can also verify that the conditions in Theorem 4.4 of Shi and Wang (2009) are also satisfied. Hence from Theorem 4.4 in Shi and Wang (2009), for the global branch $\mathcal{C}^k_\tau$, either (i) $\mathcal{C}^k_\tau$ is not compact; (ii) $\mathcal{C}^k_\tau$ contains another bifurcation point $(\hat{d_m}, 0, 1)$ for some $\hat{d_m} \neq \widetilde{d}^k_{m,\tau}$; or (iii) $\mathcal{C}^k_\tau$ contains a point $(d_m, z_1, 1 + z_2)$, where $z = (z_1, z_2) \neq 0$ and $z \in Z$, which is any complement space of $span\{(\phi_1, \psi_1)\}$. The case (ii) cannot happen as λ_1 is the only eigenvalue of K with positive eigenfunction, while all solutions on $\mathcal{C}^k_\tau$ are positive. Suppose case (iii) occurs. If $z_1 = 0$, then $z_2 = 0$ or $z_2 = -1$. But $z_2 = 0$ returns to case (ii), and $z_2 = -1$ is not possible as there is no bifurcation from the equilibrium E_0 for any $d_m > 0$.

Hence we must have that $\mathcal{C}^k_\tau$ is not compact, and indeed unbounded in $\mathbb{R}^+ \times W^{2,p}(\Omega) \times W^{2,p}(\Omega)$. From Remark 3.2, we know that the upper bound of B is $(1 + cA_2 f_\infty) + cA_2(A_3 + \delta) f_\infty := A_4$. Suppose that $(M(x), B(x))$ is a nontrivial solution of (46). It follows from $(K2)$ and $(K3)$ that

$$d_m \int_\Omega M(x)dx = \alpha e^{-d_i\tau} \int_\Omega K\left[\frac{MB}{M+w}\right]dx \le \frac{\alpha e^{-d_i\tau}}{w} \int_\Omega K\,[A_4 M]\,dx$$
$$\le \frac{\alpha e^{-d_i\tau}}{w} A_2 \max\{A_4 \int_\Omega M(x)dx, \int_\Omega \int_\Omega A_4 M(x)dxdx\}$$
$$= \frac{\alpha e^{-d_i\tau}}{w} A_2 A_4 \max\{1, |\Omega|\} \int_\Omega M(x)dx.$$

which implies that $\mathbf{proj}_{d_m}\mathcal{C}_\tau^k$ has an upper bound $\alpha e^{-d_i\tau} w^{-1} A_2 A_4 \max\{1, |\Omega|\}$. On the other hand, from Theorem 3.1, all solutions of (48) are uniformly bounded for $d_m \in [\delta, \infty)$ for any $\delta > 0$, and the boundedness in $C(\overline{\Omega})$ implies the boundedness in $L^p(\Omega)$ thus the boundedness in $W^{2,p}(\Omega)$ from L^p estimates. Therefore $\mathbf{proj}_{d_m}\mathcal{C}_\tau^k = (0, d_{m,\tau}^{*,k}]$, where $d_{m,\tau}^{*,k}$ satisfies (54). □

Similar to the bifurcation structure of constant equilibria for non-spatial model stated in Sect. 4, if $d_m'(0) \neq 0$, then a transcritical bifurcation occurs at $\widetilde{d}_{m,\tau}^k$, and the bifurcation is supercritical (or subcritical) when $d_m'(0) > 0$ (or $d_m'(0) < 0$). And the bifurcating equilibria are stable if the bifurcation is subcritical. Indeed the bifurcation analysis given here partially complements the discussion in Sect. 4 as shown in the examples given in the next section.

6 Examples and simulations

In this section, we apply the general bifurcation result in Sect. 5 to several different dispersal mappings to investigate the impact of dispersal mappings on the distributions of mistletoes and birds. In all examples we assume that the dispersal mapping K is in a form of integral operator defined in $(H2)$, and the kernel function $k(x, y) > 0$ for $(x, y) \in \overline{\Omega} \times \overline{\Omega}$. First, we consider the dispersal pattern which is uniform in space.

Example 6.1 In addition to $(H2)$, we assume that the dispersal kernel $k(x, y)$ also satisfies

$$\int_\Omega k(x, y)dy = 1, \quad \text{for every } x \in \Omega, \tag{59}$$

following Gourley and So (2002), Zhao (2009). Biologically, this means that the total dispersal of mistletoes fruit by birds from all possible locations y in the habitat Ω to a fixed location x is same for $x \in \Omega$, and the total rate is normalized to be 1. Under this assumption, one can see that all constant equilibria with delayed model (37) remain as the spatially homogeneous equilibria of (9). From (49), we get $\lambda_1 = 1$ with its corresponding constant eigenfunction $\phi_1 \equiv 1$. Hence, $\psi_1 = c/w$. Substituting these ϕ_1 and ψ_1 into (56) gives

$$d_m'(0) = \frac{\alpha e^{-d_i\tau}(c-1)}{w^2}.$$

It follows that (9) undergoes supercritical (or subcritical) transcritical bifurcation at $(0, 1)$ when $d_m = \widetilde{d}_{m,\tau}$ for $c > 1$ (or $0 \le c < 1$). In fact, the global branch $\mathcal{C}_\tau^k$ contains all constant positive equilibria described in Subsect. 4.2, hence the solution curve near the bifurcation point only contains positive constant ones. But we comment that $\mathcal{C}_\tau^k$ may contain nonconstant equilibria which are generated through secondary bifurcations, and we also notice that here the chemotactic coefficient β does not affect the local bifurcation from the line of trivial solutions $\{(d_m, 0, 1)\}$. However, we will show how β influences the stability of positive homogeneous equilibrium (M_+^τ, B_+^τ) in examples below. Finally we point out that, as shown in Chen and Shi (2011), the condition (59) is equivalent to that the constant function $\phi(x) = 1$ is the eigenfunction corresponding to the principal eigenvalue 1, and under $(H2)$, it is known that $k(x, y)$ must have the form

$$k(x, y) = 1 + \sum_{i=2}^{\infty} \lambda_i \phi_i(x)\phi_i(y), \tag{60}$$

where $(\lambda_i, \phi_i(x))$ is the eigen-pair of the Fredholm integral operator K satisfying (50), and such Fredholm integral operator K is known as Hilbert-Schmidt operator.

In the following example, we show that for the other dispersal kernels $k(x, y)$, the bifurcating equilibria shown in Theorem 5.1 are indeed spatially nonhomogeneous, and the chemotaxis can affect these equilibria.

Example 6.2 Let $\Omega = (0, \pi)$ and let $k(x, y)$ be Green's function associated with the Laplacian operator in $C^2[0, \pi]$ with Dirichlet boundary condition, i.e.

$$k(x, y) = \begin{cases} x\left(1 - \dfrac{y}{\pi}\right), & 0 \le x \le y \le \pi, \\ y\left(1 - \dfrac{x}{\pi}\right), & 0 \le y \le x \le \pi. \end{cases} \tag{61}$$

Then, we have $\lambda_1 = 1$, $\phi_1(x) = \sin x$ and $\widetilde{d}_{m,\tau}^k = \widetilde{d}_{m,\tau} = \dfrac{\alpha}{w} e^{-d_i\tau}$. Solving

$$\begin{cases} D\psi'' - \psi + \dfrac{c}{w}\phi_1 - \beta\phi_1'' = 0, \quad x \in (0, \pi), \\ \psi'(0) = \dfrac{\beta}{D}, \ \psi'(\pi) = -\dfrac{\beta}{D}, \end{cases}$$

gives

$$\psi_1(x) = A\sin x + \frac{(A - \frac{\beta}{D})\sqrt{D}}{e^{\pi/\sqrt{D}} - 1}\left(e^{x/\sqrt{D}} + e^{(\pi - x)/\sqrt{D}}\right),$$

Table 1 Parameter values used for simulations

Parameter	w	α	c	d_i	τ	D
Value	1	1	0.9	0.1	1	1

where $A = \dfrac{c+\beta w}{(D+1)w}$. From the expression (56), we obtain

$$d_m'(0) = \frac{\alpha e^{-d_i\tau}\left[-\int_0^\pi \sin^3 x dx + w\int_0^\pi \sin^2 x\psi_1(x)dx\right]}{w^2\int_0^\pi \sin^2 x dx} = \frac{8\alpha e^{-d_i\tau}(3D+1)}{3w^2\pi(4D+1)}\left[c+\beta w - \frac{4D+1}{3D+1} - \frac{3\beta D w}{4D+1}\right].$$

Thus the chemotactic effect does not change the bifurcation point $\widetilde{d}^k_{m,\tau}$, but it does affect the direction of the bifurcation of positive equilibria. Indeed, the direction of bifurcation is now determined by the quantity $c+\beta w - \dfrac{4D+1}{3D+1} - \dfrac{3\beta D w}{4D+1}$, which is a combined effort of the interaction dynamics (c), diffusion (D), and chemotaxis (β). When $c+\beta w - \dfrac{4D+1}{3D+1} - \dfrac{3\beta D w}{4D+1} > 0$, then $d_m'(0) > 0$ and the bifurcation is supercritical, and the bifurcating equilibria are unstable from Theorem 5.1. Hence larger chemotactic effect and smaller diffusion can induce bistability for some $d_m > \widetilde{d}^k_{m,\tau}$. Note that when $\beta = D = 0$, the direction of bifurcation is determined by $c-1$, again, as the non-spatial model, or the uniform kernel as in Example 6.1.

We demonstrate the effect of diffusion, bird dispersal and chemotaxis with numerical simulations. We use parameter values given in Table 1.

With these parameter values, we have $\widetilde{d}^k_{m,\tau} = \dfrac{\alpha}{w}e^{-d_i\tau} = e^{-0.1} \approx 0.9048$, and the direction of the bifurcation is determined by the quantity $c+\beta w - \dfrac{4D+1}{3D+1} - \dfrac{3\beta D w}{(4D+1)} = 0.4\beta - 0.35$. In Figs. 9 and 10, we use $\beta = 0.1$, then $d_m'(0) < 0$, and a subcritical transcritical bifurcation occurs. In this case, the mistletoes become extinct when $d_m = 0.91 > \widetilde{d}^k_{m,\tau}$ (Fig. 9), and a spatially non-homogenous equilibrium is reached when $d_m = 0.8 < \widetilde{d}^k_{m,\tau}$ (Fig. 10). On the other hand, if β is increased to 2, then $d_m'(0) > 0$, and the solution also tends to a spatially non-homogenous equilibrium for $d_m = 0.91 > \widetilde{d}^k_{m,\tau}$ (Fig. 11). This shows that chemotactic effect can be one of driving force of the spatial pattern formation. The initial values of simulations in Figs. 9, 10 and 11 are all same, and are the constant function $(M(x,t), B(x)) = (0.5, 1)$ for $t \in [-\tau, 0], x \in [0, \pi]$.

The dispersal kernel (61) shows that birds prefer to transport the fruits to the "center" part of the domain Ω, and they also prefer the shorter range dispersal rather than the longer range one. A dispersal kernel with opposite preference of birds is shown in the next example: birds are in favor of the boundary rather than the center of the domain, and they prefer the longer range dispersal than the shorter one.

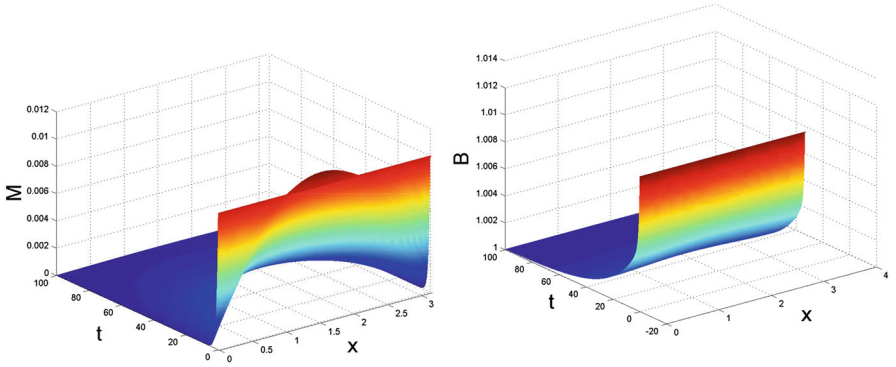

Fig. 9 Numerical simulation of (9) with $\Omega = (0, \pi)$, k is defined in (61), and parameter values are taken as in Table 1. Here $\beta = 0.1, d_m = 0.91 > \widetilde{d}^k_{m,\tau} \approx 0.9048$ and $d'_m(0) < 0$. The solution of (9) tends to $E_1 = (0, 1)$ as $t \to \infty$

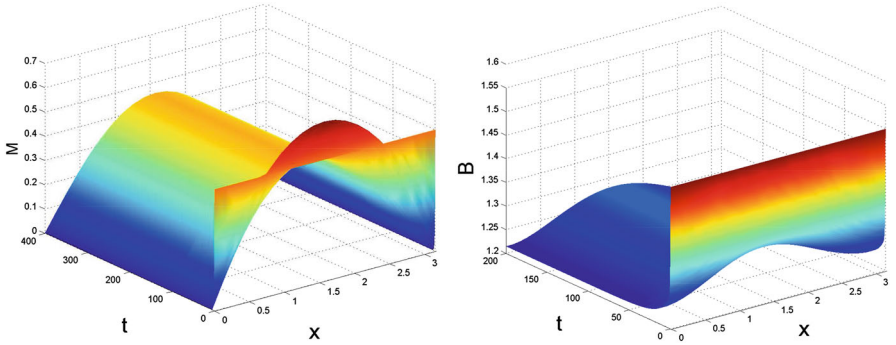

Fig. 10 Numerical simulation of (9) with $\Omega = (0, \pi)$, k is defined in (61), and parameter values are as in Table 1. Here $\beta = 0.1, d_m = 0.8 < \widetilde{d}^k_{m,\tau} \approx 0.9048$ and $d'_m(0) < 0$. The solution of (9) tends to a positive spatially nonhomogeneous equilibrium as $t \to \infty$

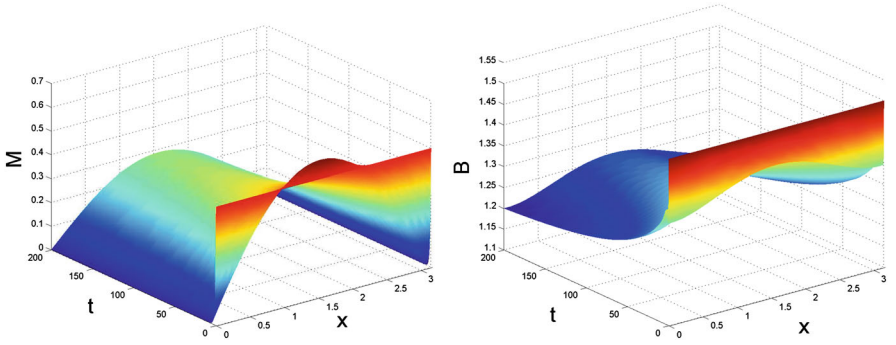

Fig. 11 Numerical simulation of (9) with $\Omega = (0, \pi)$, k is defined in (61), and parameter values are as in Table 1. Here $\beta = 2, d_m = 0.91 > \widetilde{d}^k_{m,\tau} \approx 0.9048$ and $d'_m(0) > 0$. The solution of (9) tends to a positive spatially nonhomogeneous equilibrium as $t \to \infty$

Example 6.3 Again let $\Omega = (0, \pi)$, and define

$$k(x, y) = \begin{cases} A - x\left(1 - \dfrac{y}{\pi}\right), & 0 \le x \le y \le \pi, \\ A - y\left(1 - \dfrac{x}{\pi}\right), & 0 \le y \le x \le \pi, \end{cases} \tag{62}$$

where $A \ge \pi/4$ so that $k(x, y) \ge 0$ for $(x, y) \in [0, \pi]^2$. It is straightforward to show that $(\lambda, \phi(x))$ is an eigen-pair of the associated Fredholm integral operator K if and only if

$$\begin{cases} \lambda\phi''(x) = \phi(x), & x \in (0, \pi), \\ \phi(0) = \phi(\pi), \quad A\phi'(\pi) - A\phi'(0) = \phi(0). \end{cases} \tag{63}$$

Solving (63) for $\lambda > 0$, we know that λ satisfies

$$\frac{e^{\pi/\sqrt{\lambda}} - 1}{e^{\pi/\sqrt{\lambda}} + 1} = \frac{\sqrt{\lambda}}{2A},$$

which has a unique real positive root, denoted by λ_1, and its corresponding eigenfunction is

$$\phi_1(x) = C_1 e^{x/\sqrt{\lambda_1}} + e^{-x/\sqrt{\lambda_1}},$$

Here C_1, determined by the boundary condition in (63), is given by

$$C_1 = \frac{e^{-\pi/\sqrt{\lambda_1}} - 1}{1 - e^{\pi/\sqrt{\lambda_1}}} > 0.$$

Moreover from (52), we have

$$\begin{cases} D\psi'' - \psi + \dfrac{c\lambda_1}{w}\phi_1 - \beta\phi_1'' = 0, \quad x \in (0, \pi), \\ \psi'(0) = \dfrac{\beta}{D}\phi_1'(0) = \dfrac{\beta}{D\sqrt{\lambda_1}}(C_1 - 1), \\ \psi'(\pi) = \dfrac{\beta}{D}\phi_1'(\pi) = \dfrac{\beta}{D\sqrt{\lambda_1}}(C_1 e^{\pi/\sqrt{\lambda_1}} - e^{-\pi/\sqrt{\lambda_1}}), \end{cases} \tag{64}$$

Hence

$$\psi_1(x) = C_2(C_1 e^{x/\sqrt{\lambda_1}} + e^{-x/\sqrt{\lambda_1}}) + C_3 e^{x/\sqrt{D}} + C_4 e^{-x/\sqrt{D}},$$

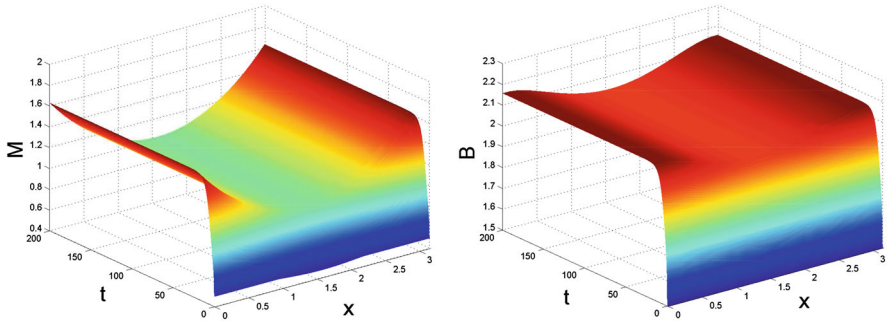

Fig. 12 Numerical simulation of (9) with $\Omega = (0, \pi)$, k is defined in (62), and parameter values are as in Table 1. Here $\beta = 0.1, d_m = 2 < \widetilde{d}^k_{m,\tau} \approx 2.1454$. The solution of (9) tends to a positive spatially nonhomogeneous equilibrium as $t \to \infty$

where

$$C_2 = \frac{\beta w - c\lambda_1^2}{(D - \lambda_1)w},$$

$$C_3 = \frac{\sqrt{D}(C_2 - \beta/D)\left[C_1(e^{-\pi/\sqrt{D}} - e^{\pi/\sqrt{\lambda_1}}) + (e^{-\pi/\sqrt{\lambda_1}} - e^{-\pi/\sqrt{D}})\right]}{\sqrt{\lambda_1}(e^{\pi/\sqrt{D}} - e^{-\pi/\sqrt{D}})},$$

$$C_4 = \frac{\sqrt{D}(C_2 - \beta/D)\left[C_1(e^{\pi/\sqrt{D}} - e^{\pi/\sqrt{\lambda_1}}) + (e^{-\pi/\sqrt{\lambda_1}} - e^{\pi/\sqrt{D}})\right]}{\sqrt{\lambda_1}(e^{\pi/\sqrt{D}} - e^{-\pi/\sqrt{D}})}.$$

A numerical simulation with the kernel defined in (62) is shown in Fig.12. Since the eigenfunctions ϕ_1 and ψ_1 both reaches their minimum in the interior, then the limiting spatially nonhomogeneous equilibrium also attain the minimum between 0 and π. The higher concentration of the limiting distribution of mistletoes and birds near the boundary reflects the mathematical property of the kernel function defined in (62).

For the final example, we consider a case that the dispersal kernel is in form $k(x, y) = f(|x - y|)$, that is, the dispersal between x and y only depends on the relative distance $|x - y|$ but not the location.

Example 6.4 Let $\Omega = (0, \pi)$, and define

$$k(x, y) = 1 - \frac{|x - y|}{\pi}, \quad 0 \le x, y \le \pi, \tag{65}$$

then the eigenvalue problem of its associated Fredholm integral operator K is equivalent to the following boundary value equation:

$$\begin{cases} \lambda\pi\phi''(x) + \phi(x) = 0, & x \in (0, \pi), \\ \phi'(0) + \phi'(\pi) = 0, \\ \phi(0) + \phi(\pi) - \pi\phi'(0) = 0. \end{cases} \tag{66}$$

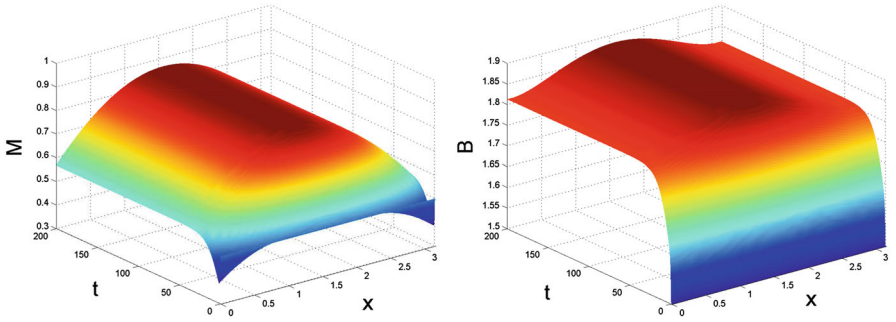

Fig. 13 Numerical simulation of (9) with $\Omega = (0, \pi)$, k is defined in (65), and parameter values are as in Table 1. Here $\beta = 0.1, d_m = 2 > \widetilde{d}^k_{m,\tau} \approx 1.9202$. The solution of (9) tends to a positive spatially nonhomogeneous equilibrium as $t \to \infty$

Direct calculation shows that (66) is solvable if and only if $\lambda = \lambda_i, i = 1, 2, \ldots$, where $\lambda_i = \dfrac{2\pi}{\theta_i^2}$, and $\{\theta_i\}_{i=1}^{\infty}$ is the increasing sequence of positive zeros of

$$f(\theta) = 2 + 2\cos\theta - \theta\sin\theta = 0.$$

In particular the principal eigenvalue of K is $\lambda_1 = \dfrac{2\pi}{\theta_1^2} \approx 2.1222$ ($\theta_1 \approx 1.7207$) with its corresponding eigenfunction

$$\phi_1(x) = (1 + \cos\theta_1)\sin\frac{\theta_1 x}{\pi} + (\theta_1 - \sin\theta_1)\cos\frac{\theta_1 x}{\pi},$$

and $\psi_1(x)$ satisfies (64) with the above ϕ_1 (we omit the algebraic form of ψ_1 here since it is too long.) A numerical simulation with the kernel defined in (62) is shown in Fig.13.

From the above examples, we can see that the dispersal kernels $k(x, y)$ have a strong impact on the limiting equilibrium distribution of mistletoes and birds. The graph of the spatially nonhomogeneous equilibrium is similar to the one of the principal eigenfunction of the corresponding Fredholm integral operator, hence determined by the kernel function $K(x, y)$. The shape of the principal eigenfunction (consequently the equilibrium) reflects the shape of kernel function to a certain extent. More precisely, the eigenfunction reaches its maximum (or minimum) in the middle if the symmetric kernel k attains its minimum (or minimum) at $y = x$ for each $x \in [0, \pi]$ (see Fig.14).

We note that for one-dimensional domain, the positive eigenfunctions are always symmetric from the uniqueness of positive eigenfunction. The limiting equilibrium distribution of mistletoes and birds are also symmetric. Indeed one can show that all stable equilibria must be symmetric, but there may exist unstable non-symmetric positive equilibria. Finally we mention that for higher dimensional spatial domain, similar spatial patterns can be observed through numerical simulations. For example, let

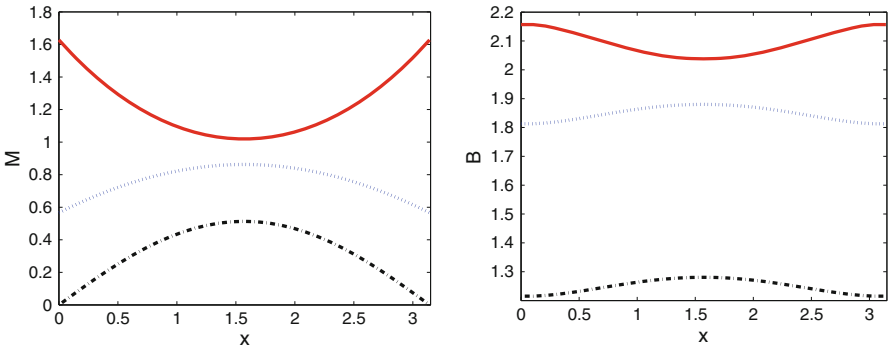

Fig. 14 The limiting equilibrium distribution of mistletoes and birds from (9) for different kernels $k(x, y)$: *solid line* (61); *dashed line* (62); *dash-dot line* (65). Here $\Omega = (0, \pi)$. *Left* mistletoes $M(x)$; *right* birds $B(x)$

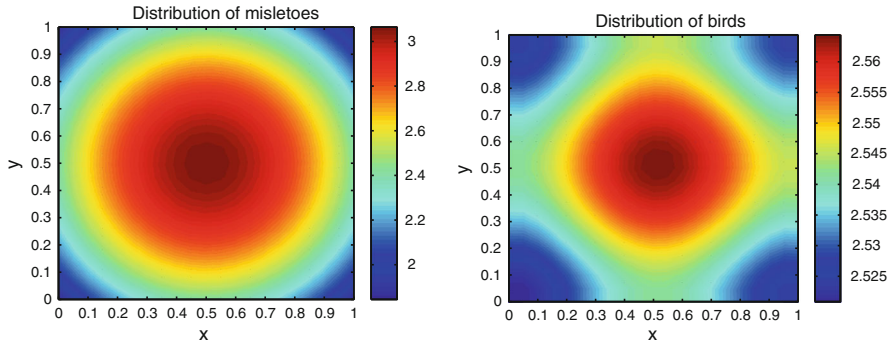

Fig. 15 Numerical simulation of (9) with k defined by (67), and parameters are as in Table 1. Here $\beta = 0.1$, $d_m = 0.7$, and the level curves of the equilibrium is plotted. The solution of (9) tends to a positive spatially nonhomogeneous equilibrium as $t \to \infty$

$$k(x, y) = \sqrt{2} - |x - y| = \sqrt{2} - \sqrt{(x_1 - y_1)^2 + (x_2 - y_2)^2}, \tag{67}$$

where $x = (x_1, x_2)$, $y = (y_1, y_2)$, and $x, y \in [0, 1] \times [0, 1]$. Then the limiting equilibrium of (9) with domain $(0, 1) \times (0, 1)$ and kernel (67) is a surface is plotted in Fig.15. Note that the distribution of mistletoes basically follows circular pattern, and the distribution of birds is similar but the shape of level curves are different due to the no-flux boundary condition.

7 Discussions and conclusions

We construct a spatially explicit model of the mutualistic interaction and dispersal of mistletoe and bird populations, or more generally, plants and their avian seed dispersers. The model characterizes their ecological behavior with a coupled system

of a reaction-diffusion-advection operator equation and a delayed operator equation. Here the operator equations often take the form of an integral form. Mathematically it is a complicated system with all these structures, but the equation is well-posed at least when the chemotactic effect is not included as proved in Theorem 3.1, and the more general case also appears to be well-posed as numerical simulations (Sect. 6) suggest that solutions always converge to an equilibrium solution. Our mathematical analysis here shows that the model possesses rich spatiotemporal dynamics with the effect of (i) maturation induced time-delay; (ii) Fickian diffusion induced by random dispersal; (iii) directed chemotactic dispersal ; and (iv) nonlocal dispersal. Moreover for certain parameter ranges, the system has a bistable structure with multiple stable equilibria, and the asymptotic dynamics could shift with the delay effect (Sect. 4.3) or chemotactic effect (Example 6.2).

An important implication of the model is the generation of an asymptotical spatial pattern of the distribution of the mistletoes and birds. Dynamically it is shown as the convergence toward an equilibrium solution. When the bird dispersal pattern is simplified to a local one (satisfying assumption $(H1)$), then the asymptotical stable equilibrium is a spatially constant one (see Sect. 4). The success/failure of the mistletoe spreading is determined by a basic reproduction number $R_0^\tau = \dfrac{\alpha}{wd_m e^{d_i\tau}}$, which quantifies the impact of the system parameters α (mistletoe attaching rate), w (functional response), d_m and d_i (mistletoe mortality rate), and τ (mistletoe mature time). Roughly speaking, when $R_0^\tau > 1$, then the mistletoe population can be established in the habitat; otherwise the mistletoe population becomes extinct while the birds live on with other food source. On the other hand, the conversion rate c from mistletoes fruits birds eaten into birds population can determine the existence of multiple positive constant equilibria. The dependence of dynamics on these parameters as well as initial conditions leads to the intricate dynamics shown in Sect. 4.

On the other hand, when the bird dispersal pattern is a nonlocal one (which is more realistic), the asymptotic positive equilibrium can no longer be a spatially homogenous one. The existence of spatially nonhomogeneous equilibrium patterns are rigorously proved with bifurcation theory (Theorem 4.3), and they are also numerically simulated for different types of dispersal kernels (Sect. 6). The bird dispersal appears in the model in the random diffusion of birds, as well as the nonlocal seed dispersal. The dispersal kernel function describes random diffusion and also other directed dispersals, but it does not describe the density dependent dispersal due to chemotactic effect, which could be done in future consideration.

While mistletoes in the model are immobile due to their ecological nature, our result shows that mistletoe population spreads via its parasitic vectors (birds). More detailed spreading dynamics of mistletoes and birds will be reported in a separate paper. On the other hand, although our model incorporates the bird population into the dispersal dynamics of mistletoes, we treat the host plant population as a constant and homogenous one. Indeed mistletoes play a dual role in ecological systems: they are mutualists of their dispersers and parasites of their host (Aukema 2003). And it has been found that seed fall more frequently on already parasitized than non-parasitized hosts. Hence an even more realistic model would be a mistletoe-host-vector system, and our work here is a step toward this ultimate goal.

Acknowledgments We are grateful to the anonymous referees for their constructive and helpful comments to improve this work. We thank Professors Mark Lewis and Yuan Lou for some helpful suggestions.

References

Alikakos ND (1979a) An application of the invariance principle to reaction-diffusion equations. J Differ Equ 33(2):201–225

Alikakos ND (1979b) L^p bounds of solutions of reaction diffusion equations. Comm Partial Differ Equ 4(8):827–868

Aukema JE (2003) Vectors, viscin, and viscaceae: mistletoes as parasites, mutualists, and resources. Front Ecol Environ 1(3):212–219

Aukema JE, Martinez del Rio C (2002) Where does a fruit-eating bird deposit mistletoe seeds? seed deposition patterns and an experiment. Ecology 83(12):3489–3496

Aukema JE (2004) Distribution and dispersal of desert mistletoe is scale-dependent, hierarchically nested. Ecography 27(2):137–144

Bannister P, Strong GL (2001) Carbon and nitrogen isotope ratios, nitrogen content and heterotrophy in New Zealand mistletoes. Oecologia 126(1):10–20

Calder M, Bernhardt P (1983) The biology of mistletoes. Academic Press, Sydney

Chang KC (2005) Methods in nonlinear analysis. Springer, Berlin

Chen S, Shi J (2011) Global attractivity of equilibrium in Gierer-Meinhardt system with activator production saturation and gene expression time delays, Submitted

Crandall M, Rabinowitz PH (1971) Bifurcation from simple eigenvalues. J Funct Anal 8(2):321–340

Crandall M, Rabinowitz PH (1973) Bifurcation, perturbation of simple eigenvalues, and linearized stability. Arch Ration Mech Anal 52(2):161–180

del Rio CM, Hourdequin M, Silva A, Medel R (1995) The influence of cactus size and previous infection on bird deposition of mistletoe seeds. Aust J Ecol 20(4):571–576

del Rio CM, Silva A, Medel R, Hourdequin M (1996) Seed dispersers as disease vectors: bird transmission of mistletoe seeds to plant hosts. Ecology 77:912–921

Gourley SA, So J (2002) Dynamics of a food-limited population model incorporating nonlocal delays on a finite domain. J Math Biol 44(1):49–78

Gourley SA, So J, Wu J (2004) Nonlocality of reaction-diffusion equations induced by delay: biological modeling and nonlinear dynamics. J Math Sci 124(4):5119–5153

Gourley SA, Wu J (2006) Delayed non-local diffusive systems in biological invasion and disease spread. In: Nonlinear dynamics and evolution equations, vol 48. Fields Institute Communications. American Mathematical Society, Providence, RI, pp 137–200

Hillen T, Painter KJ (2009) A user's guide to PDE models for chemotaxis. J. Math Biol 58(1–2):183–217

Holling CS (1959a) The components of predation as revealed by a study of small mammal predation on the European pine sawfly. Can Ent 91(5):293–320

Holling CS (1959b) Some characteristics of simple types of predation and parasitism. Can Ent 91(7):385–398

Horstmann D, Winkler M (2005) Boundedness vs. blow-up in a chemotaxis system. J Diff Equ 215(1):52–107

Hull RJ, Leonard OA (1964) Physiological aspects of parasitism in mistletoes (Arceuthobium and Phoradendron). I. The carbohydrate nutrition of mistletoe. Plant Physiol 39(6):1008–1017

Jiang J, Liang X, Zhao X (2004) Saddle-point behavior for monotone semiflows and reaction-diffusion models. J Differ Equ 203(2):313–330

Jiang J, Hi J (2010) Bistability dynamics in some structured ecological models. In: Spatial ecology. Chapman & Hall/CRC Mathematical & Computational Biology. CRC press, Boca Raton, pp 33–61

Kato T (1995) Perturbation theory for linear operators. In: Classics in mathematics. Springer, Berlin. Reprint of the 1980 edition

Kraus R, Trimborn P, Ziegler H (1995) Tristerix aphyllus, a holoparasitic loranthacea. Naturwissenschaften 82(3):150–151

Kuijt J (1969) The biology of parasitic flowering plants. University of California Press, California

Liu R, del Rio CM (2011) Spatiotemporal variation of mistletoes: a dynamic modeling approach. Bull Math Biol 73(8):1794–1811

Marshall JD, Ehleringer JR (1990) Are xylem-tapping mistletoes partially heterotrophic? Oecologia 84(2):244–248
Martin RH, Smith HL (1990) Abstract functional differential equations and reaction-diffusion systems. Trans Am Math Soc 321(1):1–44
Metz JA, Diekmann O (1983) The dynamics of physiologically structured populations. In: Lecture notes in biomathematics, vol 68. Springer, Berlin. Papers from the colloquium held in Amsterdam, 1986
Murphy DJ, Kelly D (2003) Seasonal variation in the honeydew, invertebrate, fruit and nectar resource for bellbirds in a New Zealand mountain beech forest. N Z J Ecol 27(1):11–23
Rabinowitz PH (1971) Some global results for nonlinear eigenvalue problems. J Funct Anal 7(3):487–513
Shi J, Wang X (2009) On global bifurcation for quasilinear elliptic systems on bounded domains. J Differ Equ 246(7):2788–2812
Smith HL (1995) Monotone dynamical systems: an introduction to the theory of competitive and cooperative systems. In: Mathematical surveys and monographs, vol 41. American Mathematical Society, Providence, RI
Walsberg GE (1975) Digestive adaptations of phainopepla nitens associated with the eating of mistletoe berries. Condor 77:169–174
Watson DW (2001) Mistletoe: a keystone resource in forests and woodlands worldwide. Annu Rev Ecol Syst 32:219–249
Wu J (1992) Global dynamics of strongly monotone retarded equations with infinite delay. J Integr Equ Appl 4(2):273–307
Zhao X (2009) Global attractivity in a class of nonmonotone reaction-diffusion equations with time delay. Can Appl Math Q 17(1):271–281